UNIVERSITY OF CALIFORNIA, MERCED

Modeling $\delta^{18}O$ of Phosphate and Carbonate from Recent Shark Teeth and Marine Conditions from Fossilized Shark Teeth

A Thesis submitted in partial satisfaction of the requirements

for the degree of Master of Science

in

Environmental Systems

by

Rachel Lauren Chan

Committee in charge:

Professor Sora Kim, Committee Chair
Professor Michael Beman, Examination Chair
Professor Michael Griffith

2022

Dedication Page

My thesis is dedicated to my grandparents, Harry Todd and Ellen McGuinness Todd, who have always loved me unconditionally and provided me a safe space. My papa encouraged my curiosity and rowdy behavior. I have fond memories exploring the woods behind the house, find boogie woogies in boogie woogie holes, learning how to ride a bike and drive a car, and being mad (at the time) when my skateboard was cut in half to make a rolling toolbox. My nana laid the foundations of being an independent woman and defended my mixed heritage, believing in JEDI beyond her time. Although my nana didn't go to college herself, she strongly emphasized education, from watching "Jeopardy!" to helping me with research and mixed-media creations for homework projects.

The Thesis of Rachel Lauren Chan is approved, and it is acceptable

in quality and form for publication on microfilm and electronically:

_____

Sora Kim (Committee Chair)

_____

Michael Beman (Examination Chair)

_____

Michael Griffith

_____

University of California, Merced

2022

Table of Contents

Symbols

Variables

$\delta^{18}O$: oxygen isotope value (‰)

$\delta^{18}O_{PO4}$: oxygen isotope value of phosphate (‰)

$\delta^{18}O_{CO3}$: oxygen isotope value of carbonate (‰)

$\delta^{18}O_{sw}$: oxygen isotope value of sea water (‰)

$\delta^{18}O^*_{PO4}$: predicted oxygen isotope value of phosphate (‰)

$\delta^{18}O^*_{CO3}$: predicted oxygen isotope value of carbonate (‰)

Abbreviations

Mya: million years ago

IODP: International Ocean Drilling Program

DSDP: Deep Sea Drilling Project

†: extinct species

SIA: stable isotope analysis/analyses

SIELO: Stable Isotope Ecosystem Lab of the University of California, Merced

DIC: dissolved inorganic carbon (includes CO_2, H_2CO_3, HCO_3^-, CO_3^{2-})

CMM: Calvert Marine Museum

CF – IRMS: continuous flow – isotopic ratio mass spectrometer

pH: potential (or power) of the ion hydrogen (H^+)

$[CO_3^{2-}]$: concentration of the ion carbonate (reported in unit molarity (M))

CO_2: carbon dioxide

List of Tables

List of Figures

Acknowledgements

I would like to thank my parents for flaming my rebellious side. My dad often took me to science museums, went on several adventures within and outside the country, and played the Tomb Raider franchise with me. My dad always told me to think outside the box. My mom introduced me to outdoor recreation, specifically skiing, hiking, and camping.

I would not have gotten into so many shenanigans if it weren't for my outdoor friends. TOC from TTU introduced me to rock climbing, which has taken me cross-country on many adventures. My friends from Devils Tower have provided me couches to sleep on and have come out of their way to see me in California. The Orion house in Merced was a getaway from graduate school: from mountain biking, climbing, and skiing during the day, to Smash Bros until late at night, then making aebleskivers the next morning.

I would not have gotten into graduate school if it weren't for my support in Tennessee. My mentor, Dr. Amanda Carroll, introduced me to educational outreach when I joined TTU's ACS chapter as Green Chemistry Chair. My professor, Dr. Joseph Asante, who encouraged me to take his upper-division geology classes with no geology background whatsoever and started my interest in geochemistry. My other mentor, Dr. Lauren Michel, asked me to join her stable isotope lab, take her stable isotope geochemistry course, and devoted much of her time helping me prepare graduate school applications. Much of my TTU education, including coursework and outreach, was revisited and applied for my thesis and outside projects. Despite the distance, my best friends, Anna Webb, Devyn Mitchell, and Liz Miller have been by my side since undergrad, giving me emotional support when I needed it.

SIELO has been a family for me while on my own in California during graduate school and a pandemic. Sora has provided me much guidance not only as a mentor in research, but also exploring my identity and my interests in careers. Robin has helped me work through many coding errors and statistical analysis, but also general grad student mentorship. Undergraduate students, Pedro Valencia Landa, Maya Morris, Alyssa Valdez, and Andrea Lee have helped me immensely with weighing samples and let me be a mentor. My close friends and lab mates Molly Karnes, Gina Palefsky, Corey Shaver, Anna Jurusik, Gabriele Larocca-Conte, Jon Kuntz, Laura van Vranken, Mario Hernandez, and Hannah Palmer – you guys have helped with the process of writing this thesis, from providing edits and ideas, helping me understand mental health better, mentorship, and making me feel seen.

I also want to thank and acknowledge my committee, funding source, and institutions that supported my thesis. My committee members include Sora, Michael Beman, and Michael Griffiths, who provided much feedback, ideas, and directions this thesis could go. This project brought many of my scientific interests together, while allowing me to grow and appreciate new areas. The National Science Foundation funded this project and provided me a stipend the last few years. The Calvert Marine Museum provided my fossilized tooth samples, and students from William Patterson University powdered most of the teeth before I arrived to California.

Finally, I want to thank my beans. My sweet bean, Cole Cooper, and my toe bean, Tobi. Thank you for letting me be my weird self and being weird with me. You two have made me love and laugh.

Abstract

Modeling $\delta^{18}O$ of Phosphate and Carbonate from Recent Shark Teeth and Marine Conditions from Fossilized Shark Teeth

by

Rachel Lauren Chan

Master of Science in Environmental Systems

University of California, Merced, 2022

Research Advisor: Sora Kim

The Neogene (~23.0 – 2.6 million years ago) is the current climate analogue used in predictive scenario modeling, as it is characterized as having similar biota, geography, and environments when compared to present-day. Parameters that cannot be directly measured from the past can be estimated by stable isotope analysis measurements from proxies. Unlike most marine proxies, shark teeth provide 'snapshots' of environmental conditions during formation. Shark teeth can be used to calculate sea temperatures the teeth formed in after measuring $\delta^{18}O$ of phosphate (PO_4) and carbonate (CO_3) within the enameloid and using $\delta^{18}O$ of seawater ($\delta^{18}O_{sw}$) estimates. Here, we model $\delta^{18}O_{PO4}$ and $\delta^{18}O_{CO3}$ from published linear regression equations to assess the fidelity of local T and $\delta^{18}O_{sw}$ being recorded in modern shark teeth. We also developed a Bayesian regression model to estimate the probability of T and $\delta^{18}O_{sw}$ for basins using $\delta^{18}O_{PO4}$ of fossilized Neogene shark teeth from our collection and published datasets. Modern empirical $\delta^{18}O$ and predictive $\delta^{18}O$* values indicate that carbonate (mean = 27.4 ± 1.5‰) is not a reliable recorder and therefore should not be considered as a paleothermometer until further constrained, but phosphate (mean = 23.5 ± 0.7‰) $\delta^{18}O_{PO4}$ values were similar between taxa at localities and suggest a latitudinal temperature gradient. Variation within and between taxa may be due to species specific migration and mesothermy. Neogene T and $\delta^{18}O_{sw}$ estimates reflect a warmer climate, and salinity and temperature differences between the Miocene and Pliocene epochs.

1. INTRODUCTION

The Neogene (Miocene-Pliocene epochs) was a time of climate fluctuation with decreasing temperatures, *p*CO2, and sea levels as glaciation increased. The continents were nearly in their modern configurations and ocean currents shifted to modern circulations as oceanic gateways opened or closed. The Neogene (23.0 – 2.58 million years ago [Mya]) was relatively similar in terms of biota, environment, and geography, albeit cold trending due to orbital forcing (Holbourn et al., 2013; Miller et al., 2020; Zachos et al., 2001). The similarities between the Neogene and today make it a suitable analogue for modeling, as past climates present scenarios to model future climates. Since conditions in the Neogene were analogous to today, there have been a number of studies estimating global climate over geologic timelines but understanding smaller scale interactions between the environment and ecology distinguishes nuances at local or regional levels. Reconstructions of this scale require a proxy that captures these subtle signals.

Paleoceanographic studies rely on climate indicators, often from calcareous foraminifera, which record global deep-sea and surface temperatures via oxygen isotope and Mg/Ca composition. However, foraminifera archives are a temporal 'panorama' of geologic time (Pearson, 2012) and often located in low- and mid-latitudes since these are optimal for International Ocean Drilling Program (IODP) and Deep Sea Drilling Project (DSDP) sites. Other invertebrate records with distributions spanning latitude and depth are also used as paleoceanographic proxies. Mollusks, coral, and nannoplankton serve as substrates in temperate and tropical environments while siliceous diatoms can track upwelling zones and cold, high latitude regions (Steinthorsdottir et al., 2021; Wierzbowski, 2021). Studies have also analyzed fossil vertebrates (i.e., fish, sharks, cetaceans, etc.) for stable isotope analysis to reconstruct environmental conditions, but these are often limited to localities or regions (Steinthorsdottir et al., 2021). When using biological organisms as paleoceanographic proxies, it is important to consider their ecology, which is intrinsically linked to how they record the environment.

Shark teeth are complementary proxies to invertebrates in elucidating paleoceanography, as they provide a broader "snapshot" of environment and are spatiotemporally abundant. First, shark teeth record marine conditions during their formation and mineralization (Vennemann et al., 2001; Vennemann & Hegner, 1998). It is thought that shark body water is in equilibrium with ambient water (Vennemann et al., 2001) and incorporates on short time scales during mineralization with odontogenesis (Zeichner et al., 2017). Second, sharks (Chondrichthyes) are distributed globally and at depth, being rich at mid-latitudes in the epipelagic zone along the coast and continental shelves but also inhabiting northern high-latitude, brackish or freshwater (Lucifora et al., 2011). During past periods of greenhouse conditions (i.e., Eocene [56 – 33.9 Mya]), †*Striatolamia macrota* flourished from the Southern Ocean of Antarctica to the Arctic Ocean (Kim et al., 2020). Third, shark teeth are regularly shed and replaced throughout the lifespan of a shark, making them prolific throughout the fossil record. The oldest tooth specimen found has been dated to the Lower Devonian (~419.2 - 393.3Ma) (Botella et al., 2009), potentially capturing environmental proxy data beyond ocean sediment cores.

Many paleothermometers rely on oxygen isotope analysis from biogenic inorganic carbonate (CO_3^{2-}) and phosphate (PO_4^{3-}). Shark teeth contain two mineralized components, dentine and enameloid, that include both CO_3 and PO_4 groups. Dentine is primarily hydroxyapatite ($Ca_5(PO_4, CO_3)OH$) and useful for contemporary isotope analyses, but it is prone to degradation due to its high organic (~20-30%) content (Carlson, 1991; Enax et al., 2012; LeGeros, 1981). In contrast, enameloid is composed of fluorapatite ($Ca_5(PO_4, CO_3)F$), which is compact, low in solubility (both when increasing temperature and decreasing pH), and highly inorganic (~99% by weight) (Enax et al., 2012, 2014; LeGeros, 1990; LeGeros, 1981; Leung et al., 2022; Miake et al., 1991; Posner et al., 1984). The characteristics of fluorapatite make enameloid highly resistant to diagenesis, the process which fossils become either chemically, physically, or biologically altered post-mortem (Keenan, 2016), making the outer layer an ideal proxy material for stable isotope analyses (SIA).

More recently, shark teeth have been suspected of recording regional conditions rather than the locality teeth were found. Earlier studies by Vennemann et al. (1998, 2001, 2002) using SIA of shark teeth drew environmental inferences based on where teeth are retrieved, rather than where they potentially mineralized. These studies do not necessarily account for species' migration habits, which has been difficult to map until relatively recently. Telemetric tagging has improved our understanding of extant shark movement patterns (Hammerschlag et al., 2011) and environmental temperature during migration (Teo et al., 2004; Teter et al., 2015). Seasonal migrations for sharks are influenced by prey availability and/or thermal regime as most species are ectothermic. This migration-temperature coupling influences the oxygen isotopic composition of shark enameloid, which has been mentioned in reconstructive studies using shark teeth (Aguilera et al., 2017; Amiot et al., 2008; Barrick & Fischer, 1993; Fischer et al., 2013; S. L. Kim et al., 2020; Kocsis et al., 2007; Pellegrini & Longinelli, 2008; Roelofs et al., 2017), but has not been investigated until this study. Further, this phenomenon has been demonstrated in $\delta^{18}O$ values of modern and fossilized fish teeth (excluding sharks) (Sisma-Ventura et al., 2019). While not specifically $\delta^{18}O$, (Shipley et al., 2021) demonstrated that movement patterns influence $\delta^{13}C$ and $\delta^{15}N$ values in the dental collagen of modern shark teeth. Some migratory shark species are also mesothermic (such as *Carcharodon carcharias*), meaning the species can temporarily elevate body temperatures (Bernal et al., 2012); the impact of mesothermy on oxygen isotope composition of enameloid is largely unknown. We explore this coupling between migration and temperature with respect to stable isotope composition, as more consideration will improve temperature estimates for environmental reconstructions.

While the literature considers both carbonate and phosphate oxygen in enameloid to be in equilibrium with body water, the carbonate oxygen isotope composition is probably more nuanced. Recent studies indicate that carbonate isotope composition likely reflects a combined diet, metabolic, and dissolved inorganic carbon (DIC) signal (Karnes, 2022; Sisma-Ventura et al., 2019). (Vennemann et al., 2001) found that carbonate $\delta^{18}O$ values in enameloid have more variation than phosphate $\delta^{18}O$ values and are likely not in isotopic equilibrium with seawater, which is thought to be in steady state with aquatic ectotherms. To date, there has been no controlled experiment determining vital effects

seen in $\delta^{18}O_{CO3}$ and possibly $\delta^{18}O_{PO4}$ values of shark teeth, potentially producing inaccurate temperature and salinity reconstructions.

Here, we determine the fidelity of marine temperature and salinity estimates by examining paired analyses of $\delta^{18}O_{CO3}$ and $\delta^{18}O_{PO4}$ values from shark enameloid of extant and fossilize Neogene specimens. First, we analyze $\delta^{18}O_{CO3}$ and $\delta^{18}O_{PO4}$ values from extant sharks, then predict $\delta^{18}O_{CO3}$ and $\delta^{18}O_{PO4}$ values for these specimens based on environmental conditions where they were caught to evaluate the fidelity of shark teeth as environmental recorders using the (Kolodny et al., 1983) linear regression equation. Then, we explore the potential of fossil specimens to elucidate temperature gradients during the Neogene. In addition to analyzing specimens from California (USA), North Carolina (USA), and Peru, we also compiled published phosphate oxygen isotope data. Based on $\delta^{18}O_{PO4}$ values binned by geological age, latitude, and ocean basin, we estimated water temperature and isotopic composition of Neogene localities using a Bayesian model based on measured $\delta^{18}O_{PO4}$ values from fossilized teeth. This Bayesian model reconstructs probable regional condition changes in oceanography that occurred during the Miocene-Pliocene transition. The Bayesian regression model used the Neogene as a case study, but has the potential reconstruct sea temperatures and $\delta^{18}O_{sw}$ from other geologic time periods with possibly complementary proxies.

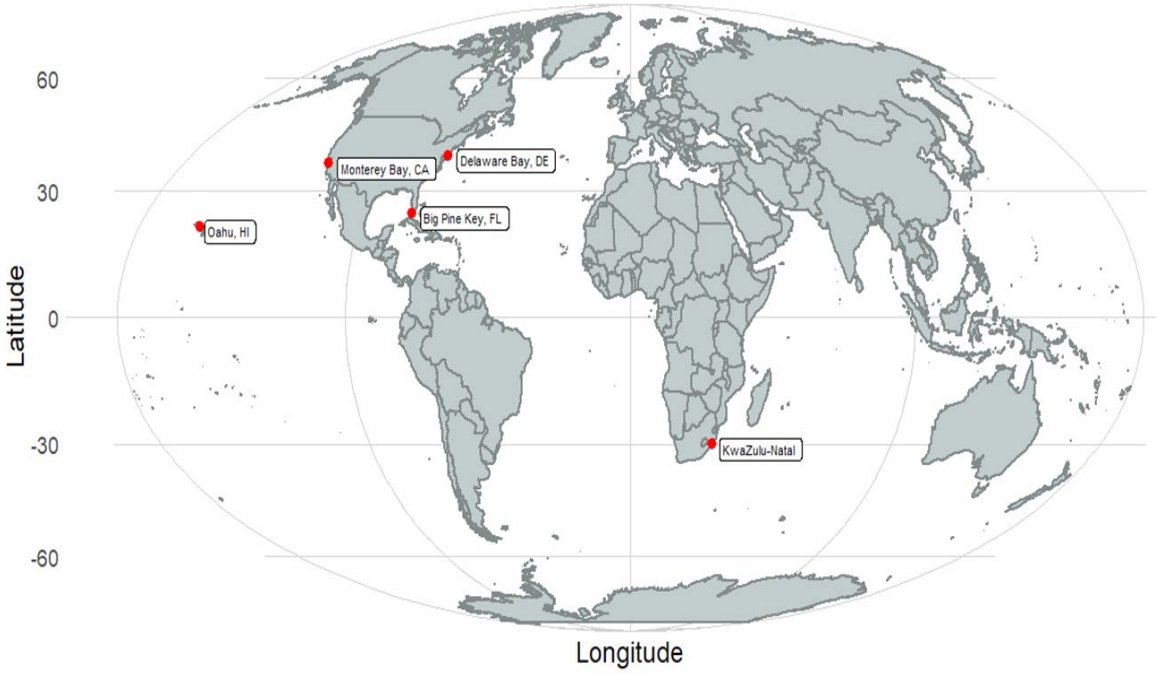

Figure 1. Map of modern teeth collection sites.

2. METHODS

Extant shark teeth are from multiple taxa and localities **(Fig 1, Table 1)**. Fossilized teeth are from Neogene localities in California (USA), North Carolina (USA), and Peru **(Fig 2, Table 2)**. All extant and fossil teeth sampled in this study are in the Calvert Marine Museum collections (CMM).

2.1 Sampling Preparation

We powdered the enameloid from several species of modern sharks and specimens from Miocene through the Pliocene. A slow speed Dremel dental drill equipped with a 300µm diamond-tipped bit abraded the enameloid. Before isotopic preparation, 4.0 - 5.0mg of enameloid powder weighed and residual organics removed with 1.0mL 3% NaOCl overnight. The solution was discarded, and remaining powder was rinsed five times with deionized water (DIW), then dried overnight in an oven set to 50°C.

2.2 Isotope Analyses

For this study, the enameloid of extant and fossil specimens was powdered and prepared for SIA of $\delta^{18}O$ values from the phosphate- and carbonate-bound groups of fluorapatite. Stable isotope composition of oxygen was analyzed at the Stable Isotope Ecosystem Lab of UC Merced (SIELO) with a Delta V Plus continuous flow isotope ratio mass spectrometer (CF-IRMS).

2.2.1 Carbonate Chemistry and Analysis

We subsampled 3.0 - 4.0 mg of enameloid powder for carbonate isotope preparation. To remove secondary carbonates, samples reacted with a buffered solution of 0.91M calcium acetate and 1.0M acetic acid (pH ~5) at 4°C for 24hrs. Powders were rinsed five times with DIW and dried at 50°C overnight in an oven.

Carbonate samples were weighed to 1.0mg for carbonate isotope analysis. Atmospheric air was removed by flushing samples with He gas in exetainers. Then, a 1.0mL of 104% H_3PO_4 was added and samples digested at 27°C for 1 hour. The headspace of the exetainers was sampled for CO_2 using a GasBench coupled to a Delta V Plus CF-IRMS with a Conflo IV. We used calibrated reference materials for $\delta^{18}O_{CO3}$ corrections that included drift and linearity (Carrara Marble [n = 38, $\delta^{13}C$ = 2.1 ± 0.21‰, $\delta^{18}O$ = -2.0 ± 0.22‰]; NBS 18 [n = 38, $\delta^{13}C$ = -4.9 ± 0.28‰, $\delta^{18}O$ = -23.2 ± 0.15‰]; USGS 44 [n = 39, $\delta^{13}C$ = -41.9 ± 0.37‰], $\delta^{18}O$ = -15.6 ± 0.15‰]).

2.2.2 Phosphate Chemistry and Analysis

For phosphate analysis, powders were subsampled (1.0 – 1.5mg) to precipitate Ag_3PO_4 using the UC rapid phosphate precipitation protocol by Mine et al. (2017). These subsamples were dissolved in 50µL of 2.0M HNO_3 overnight. The following day, Ca^{2+} and PO_4^{3-} were ionized by adding 30µL of 2.9M HF and 50µmL of 2.0M NaOH. The solution was agitated for 2hrs to pellet CaF_2. The supernatant containing PO_4^{3-} was transferred to a separate microtube and the remaining pellet was rinsed 50µL with 0.1M NaF for remaining PO_4^{3-}. Supernatants were combined and Ag_3PO_4 was precipitated by adding 180µL of Ag-amine solution (1.09M NH_4OH and 0.37M $AgNO_3$. To completely precipitate Ag_3PO_4 and prevent isotopic fractionation of oxygen, the pH window (approximately 5.5 to 7.5) was adjusted with 2.0M HNO_3 (approximately 10µL aliquots) and allowed to react for 10min. Crystals were centrifuged to pellet, rinsed five times with DIW, then dried in the oven overnight at 50°C.

For the stable isotope composition of phosphate-oxygen ($\delta^{18}O_{PO4}$), we triplicated subsamples and weighed to 0.15-0.20mg in silver capsules. Instrumental analysis was performed on a TCEA coupled with a Delta V Plus CF-IRMS with a Conflo IV. We used calibrated reference materials (USGS 80 [n = 55, $\delta^{18}O$ = 13.2 ± 0.37‰]; USGS 81a [n = 52, $\delta^{18}O$ = 35.4 ± 0.37‰]; IAEA 601 [n = 28, $\delta^{18}O$ = 23.1 ± 0.63‰]) and standard preparation materials (NIST 120C, hydroxyapatite).

2.3 Published $\delta^{18}O$ metadata

We conducted a literature review of published $\delta^{18}O$ values of shark teeth across the Neogene to supplement our dataset **(Table 3)**. Google Scholar was searched with terms "oxygen isotope", "shark enameloid", "Neogene", "Miocene", and "Pliocene". The $\delta^{18}O$ values included oxygen isotopes from both carbonate and phosphate groups within enameloid. We only included $\delta^{18}O$ values of enameloid in our literature review since $\delta^{18}O$ values of dentine or whole tooth may be influenced by organic material, which is more susceptible to alteration (Vennemann et al., 2001).

2.4 Modeling $\delta^{18}O$ from Modern Teeth and Marine Conditions from Fossil Teeth

2.4.1 Modeling Modern $\delta^{18}O_{PO4}$ and $\delta^{18}O_{CO3}$ Values

We compared empirical and predicated isotope composition using various models that consider temperature and source water $\delta^{18}O$ values. First, we created a normal distribution loop iteration for sea surface temperature (SST) and assumed seawater (SW) to be in steady state with the enameloid-forming source water ($\delta^{18}O_{sw}$; i.e., body water). Temperature data was collected from NOAA's National Data Buoy Center (NOAA, 1971) and $\delta^{18}O_{sw}$ was determined from NASA's Global Seawater Oxygen-18 Database (Schmidt et al., 1999). For temperature, data was retrieved from the nearest buoy with months sharks reside for the locality. The $\delta^{18}O_{sw}$ data was retrieved based on locality coordinates. Temperature and $\delta^{18}O_{sw}$ is averaged based on time sharks inhabit the locality. If locality data could not be retrieved from these databases, we used affiliated databases or published values. For both the fractionation equations, we use the same modern SST and $\delta^{18}O$ values for each locality. Second, the locality's normal distribution of SST and $\delta^{18}O_{sw}$ value is averaged to calculate the mean mineral oxygen isotope composition of teeth. For phosphate, we used the Kolodny et al. (1983) apatite-phosphate equation, recalibrated by Lécuyer et al. (2013), and rearranged to solve for $\delta^{18}O^*_{PO4}$.

$$\delta^{18}O^*_{PO4} = \delta^{18}O_{sw} - \frac{(T - 119.3)}{4.38} \quad \text{Eqn 1}$$

Where $\delta^{18}O^*_{PO4}$ is the mean predicted oxygen isotope composition of phosphate, $\delta^{18}O_{sw}$ is averaged oxygen isotope composition of water, and T is the average water temperature in Celsius. For carbonate, we used the calcite-water fractionation factor equation by O'Neil et al. (1969), rearranged to solve for α.

$$1000 \ln \alpha = 2.78(10^6 T^{-2}) - 3.39 \quad \text{Eqn 2}$$

Where α is the fractionation factor between calcite and water, and T is the average water temperature in Kelvin. The α factor is used to solve for the oxygen isotope composition of carbonate.

$$\delta^{18}O^{*}_{CO3} = \alpha(\delta^{18}O_{sw} + 1000) - 1000 \quad \text{Eqn 3}$$

Where $\delta^{18}O^{*}_{CO3}$ is the mean predicted oxygen isotope composition of carbonate. We then compare the proximity of predicted $\delta^{18}O^{*}$ to the average empirical mineral $\delta^{18}O$ value **(Table 1)**. This model was coded in R (code available in supplementary file).

2.4.2 Estimating Neogene Sea Temperature and $\delta^{18}O_{sw}$ Values

We developed a Bayesian regression model to estimate Miocene and Pliocene temperature and $\delta^{18}O_{sw}$ values from shark teeth $\delta^{18}O_{PO4}$ values. We assumed a normal distribution of $\delta^{18}O_{PO4}$ around mean μ, with standard deviation σ.

$$\delta^{18}O_{PO4} \sim N(\mu, \sigma) \quad \text{Eqn 4}$$

Where μ is determined by the relationship among T (°C), $\delta^{18}O_{sw}$, and $\delta^{18}O_{PO4}$ as proposed by (Longinelli & Nuti, 1973) and the dispersion term (σ) is estimated from the data.

$$\mu = \delta^{18}O_{sw} - \frac{T - 119.3}{4.38} \quad \text{Eqn 5}$$

Table 1. Modern empirical $\delta^{18}O$ values for localities from shark taxon compared to predicted ($\delta^{18}O^{*}$) values. Blank $\delta^{18}O$ boxes indicate that the PO_4 and CO_3 values are the same as the locality values. μ_{PO4} values are reported in VSMOW, while μ_{CO3} are VPDB.

Locality (latitude)	Locality mean (‰)	Taxon	n^{PO4}	n^{CO3}	$\delta^{18}O_{PO4}$ (‰)	$\delta^{18}O_{CO3}$ (‰)	$\delta^{18}O^{*}_{PO4}$ (‰)	$\delta^{18}O^{*}_{CO3}$ (‰)
Big Pine Keys, FL (24.7° N)	μ_{PO4} = 23.0 ± 0.3 μ_{CO3} = -3.1 ± 1.4	*C. limbatus*	5	3	23.0 ± 0.34	-4.1 ± 1.4	22.5 ± 0.8	-1.5 ± 0.7
		C. obscuras	5	5	23.0 ± 0.2	-2.5 ± 1.1	21.8 ± 0.8	-2.2 ± 0.8
Delaware Bay (39.1° N)	μ_{PO4} = 23.7 ± 0.68 μ_{CO3} = -4.0 ± 1.0	*C. taurus*	39	39	23.7 ± 0.7	-4.0 ± 1.0	23.0 ± 0.5	-1.1 ± 0.5
KwaZulu-Natal (28.5° S)	μ_{PO4} = 23.0 ± 0.3 μ_{CO3} = -2.6 ± 1.1	*C. leucas*	10	15	22.9 ± 0.3	-3.0 ± 0.8	21.9 ± 0.5	-2.1 ± 0.5
		S. mokarran	-	4	-	-3.1 ± 2.0	21.9 ± 0.6	-2.1 ± 0.5
		G. cuvier	-	9	-	-2.3 ± 0.7	21.9 ± 0.7	-2.1 ± 0.5
		C. carcharias	6	6	23.1 ± 0.2	-1.6 ± 0.6	21.9 ± 0.8	-2.1 ± 0.5
Oahu, HI (21.4° N)	μ_{PO4} = 24.0 ± 0.4 μ_{CO3} = -0.9 ± 0.1	*O. ferox*	3	3	24.0 ± 0.4	-0.9 ± 0.1	23.5 ± 0.5	-0.7 ± 0.5
Monterey Bay, CA (36.9° N)	μ_{PO4} = 23.7 ± 0.3 μ_{CO3} = -1.5 ± 0.5	*L. ditropis*	3	3	23.7 ± 0.34	-1.3 ± 0.5	24.0 ± 0.4	-0.1 ± 0.4
		C. carcharias	0	1	-	-1.9	24.0 ± 0.5	-0.1 ± 0.4

Bayesian models attempt to estimate the probable values of unknown parameters (in our case, Neogene temperature and $\delta^{18}O_{sw}$) based on data ($\delta^{18}O_{PO4}$) and prior knowledge of these parameters. This relationship is formalized in Bayes' theorem where:

$$P(T,\ \delta^{18}O_{sw}|\delta^{18}O_{PO4}) = \frac{P(\delta^{18}O_{PO4}|T,\ \delta^{18}O_{sw})}{\delta^{18}O_{PO4}}\ x\ P(T,\ \delta^{18}O_{sw}) \quad \text{Eqn 6}$$

The first term on the right-hand side of equation 6 is known as the likelihood and is the conditional probability of our data, given a proposed temperature and $\delta^{18}O_{sw}$ value. The second term represents our prior beliefs about these parameters. Since sharks have clear habitat temperature preferences, we define the prior probability of temperature as $T \sim \mathcal{U}(5, 30)$ which essentially covers the predilection temperature range of all modern sharks species (Grady et al., 2019). We also defined the prior probability of $\delta^{18}O_{sw}$ as $\delta^{18}O_{sw} \sim \mathcal{N}(\mu = -0.5, \sigma = 0.5)$, which is the variability of a well-mixed ocean with a slightly more negative mean to reflect melting of polar ice volume in the Miocene and Pliocene (Billups, 2002; Lear et al., 2000). Combining these equations gives the final joint probability of:

$$P(T,\ \delta^{18}O_{sw}|\delta^{18}O_{PO4}) = \text{N}(\mu, \sigma) \text{ x U}(5, 30) \text{ x N}(-0.5, 0.5) \quad \text{Eqn 7}$$

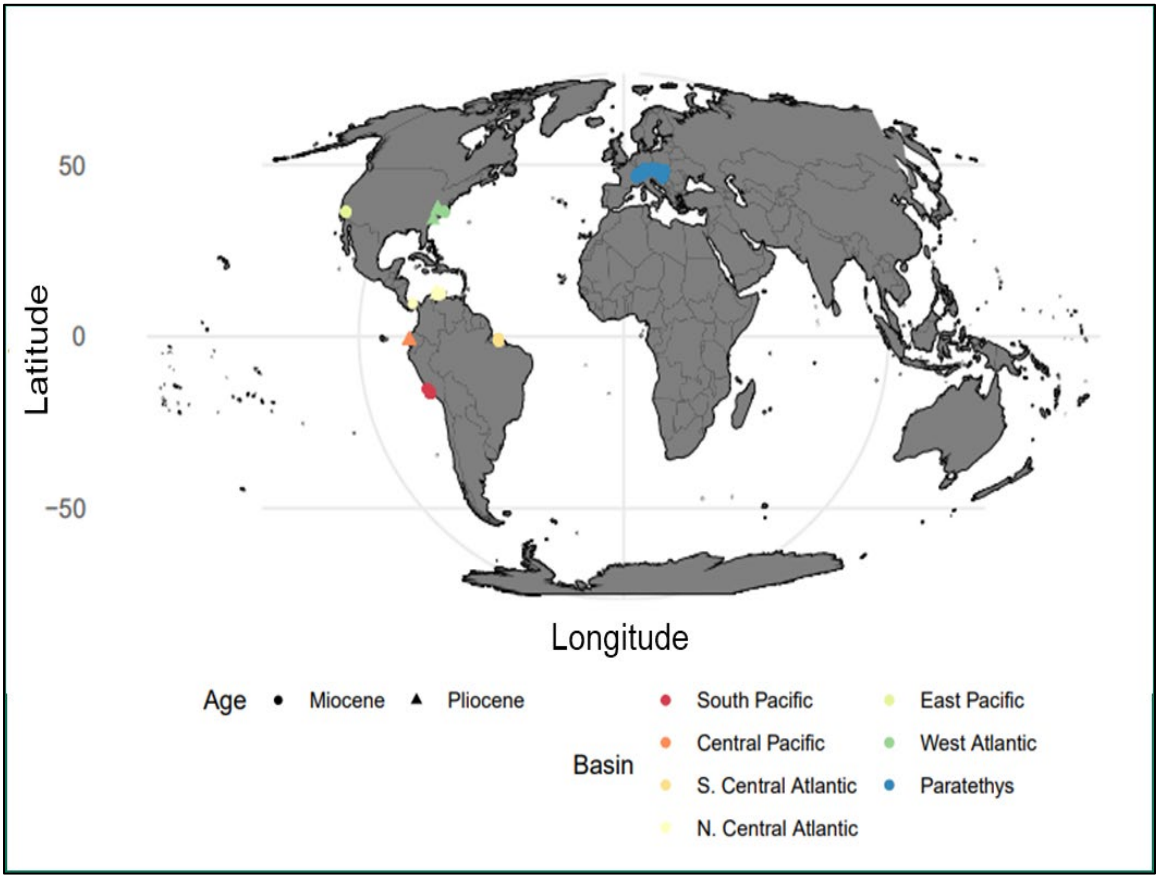

Figure 2. Map of Neogene basins.

To estimate each parameter, we used Markov Chain Monte Carlo with an adaptive Metropolis algorithm (Haario et al., 2001). We binned $\delta^{18}O_{PO4}$ data by latitude, age, and ocean basin (**Table 4, Figure 5**).

Table 2. Original collection sites of this study's Neogene specimens from CMM.

Basin	Locality	Formation	Epoch	Age	Exact Age
East Pacific	Santa Cruz CA, (USA)	Purisma	Pliocene	Zanclean	~5.3 - 3.6Ma
	Bakersfield CA, (USA)	Temblor	Miocene	Langhian	~16.0 - 13.7Ma
West Atlantic	Aurora Region NC, (USA)	Yorktown	Pliocene	Piazencian	~3.6 - 2.6Ma
		Pungo River	Miocene	Langhian	~16.0 - 13.7Ma
South Pacific	Pisco, Peru	Pisco	Miocene	Messinian to Tortonian	~11.6 - 5.3

Table 3. Compiled Neogene $\delta^{18}O_{PO4}$ values from published studies.

Basin	Publication	Epoch
South Central Atlantic	*Aguilera et al. (2017)*	Miocene
North Central Atlantic	*Aguilera et al. (2017)* *Carrillo-Briceño et al. (2019)*	Miocene to Pliocene
South Pacific	*Amiot et al. (2008)*	Miocene
Central Pacific	*Pelligrini and Longinelli (2008)*	Pliocene
Paratethys	*Kocsis et al. (2007)* *Kocsis et al. (2009)* *Vennemann et al. (1998)*	Miocene

3. RESULTS

3.1 Phosphate and Carbonate Empirical Values

Modern species from localities of similar latitude have similar $\delta^{18}O_{PO4}$ values (**Table 1, Fig 3**). Teeth from lower mid-latitudes (Big Pine Keys, FL ($\delta^{18}O_{PO4}$ mean = 23.0 ± 0.3‰) and KwaZulu-Natal, South Africa ($\delta^{18}O_{PO4}$ mean = 23.0 ± 0.3‰)) had the lowest mean $\delta^{18}O_{PO4}$ values, and teeth from middle mid-latitudes (Monterey Bay, CA ($\delta^{18}O_{PO4}$ mean = 23.7 ± 0.3‰)and Delaware Bay, USA ($\delta^{18}O_{PO4}$ mean = 23.7 ± 0.7‰)) had higher mean $\delta^{18}O_{PO4}$ values. Teeth from Hawaii had the highest $\delta^{18}O$ phosphate values ($\delta^{18}O_{PO4}$ mean = 24.0 ± 0.4‰). We do not see similar results with measured mean $\delta^{18}O_{CO3}$ teeth values at the local or taxa level. The range and variation of $\delta^{18}O_{PO4}$ values were more distinct between modern and fossil teeth. Neogene-aged teeth had mean $\delta^{18}O_{PO4}$ values of 20.9 ± 1.5‰ and had a range of 10.3‰ to 24.1‰, whereas modern samples had mean $\delta^{18}O_{PO4}$ values of 23.5 ± 0.7‰ and range of 21.9‰ to 24.8‰.

Fossilized teeth from the Neogene show similar range and variation of $\delta^{18}O_{CO3}$ (**Fig 4**) values when compared to modern values. Fossil teeth (n = 401) have $\delta^{18}O_{CO3}$ range from 20.9 to 28.2‰ and mean of 25.7 ± 1.4‰. The modern sampled teeth (n = 118) have higher $\delta^{18}O_{CO3}$ values by 2.0‰, ranging from 22.6‰ to 30.9‰ and mean of 27.4 ± 1.5‰.

3.2 Phosphate and Carbonate Model Predictions

We compared predicted phosphate and carbonate $\delta^{18}O$ values (denoted as $\delta^{18}O^*_{PO4}$ and $\delta^{18}O^*_{CO3}$, respectively, in **Table 1**) to empirical enameloid values (denoted as $\delta^{18}O_{PO4}$ and $\delta^{18}O_{CO3}$, respectively) in order to evaluate if conditions could be used to predict the oxygen isotope composition in shark teeth (**Fig 3**). The Kolodny et al. (1983) equation (**Eqn 1**) predicted values that were generally offset by approximately 2.0 – 2.5‰ from the empirical $\delta^{18}O_{PO4}$ value, while the O'Neil et al. (1953) equation (**Eqn 2**) had prediction offsets that were inconsistent. The linear regression between empirical and predicted for phosphate $\delta^{18}O$ values was $y = 0.4713x + 12.6365$, a $r^2 = 0.74$, and a p-value of 0.01, while carbonate had a regression of $y = 0.5823x – 1.6687$, a $r^2 = 0.21$, and a p-value of 0.19. The phosphate equation has greater correlation (r^2), less variation of $\delta^{18}O$ than the carbonate equation, and greater significance.

Hawaii and Delaware Bay had anomalous predictions based on conditions where the tooth was collected (extracted or found). For these two localities, the predicted averages of both phosphate and carbonate were outside our 95% confidence interval. We ran the model again using temperatures where we believed teeth formed, such as North Carolina for Delaware Bay and cooler temperature to reflect depth for Hawaii. Interestingly, this North Carolina $\delta^{18}O^*_{CO3}$ value was a better estimate than its $\delta^{18}O^*_{PO4}$ counterpart (19.0 ± 0.7‰), which had an offset of approximately 6‰ when using temperature and $\delta^{18}O_{sw}$ from. Hawaii $\delta^{18}O^*_{CO3}$ estimations were outside the confidence interval, but the estimation (-0.7 ± 0.5‰) made for conditions likely during tooth development was nearly on the one-to-one line.

3.3 Latitudinal Gradient

Spatially, our set of Neogene-aged teeth span the Pacific and Atlantic Oceans and Paratethys Sea from equatorial to mid-latitudes (**Fig 2**). Collected teeth from the Miocene are widely distributed. The Pacific is more disbursed, having localities at low- and mid- latitudes on the western coasts of the American continents, while localities in the Atlantic are found from central- to mid-latitudes. All Paratethys teeth localities were from the western area of the basin. The Pliocene is sparser, with equatorial teeth in the Pacific, and central and mid-latitude in the Atlantic. No phosphate teeth values from the Pliocene have been collected for the Paratethys to our knowledge.

We estimated temperatures based on the Bayesian regression model (**§2.4.2**) based on measured $\delta^{18}O_{PO4}$ values from teeth that were binned by latitude, ocean basin and age, $\delta^{18}O_{sw}$ estimations of the Neogene from the literature, and prior temperatures from extant sharks (Grady et al., 2019). The Atlantic averaged 24.1 ± 2.1°C at north-central locality, 25.0 ± 0.4°C at the south-central locality, and 13.7 ± 3.2°C at the north-western locality. The southern Pacific averaged 15.3 ± 2.3°C than modern average temperature at latitude, whereas the north-eastern Pacific averaged at 15.1 ± 3.3°C. The Paratethys is estimated to have been at 17.5 ± 2.4°C.

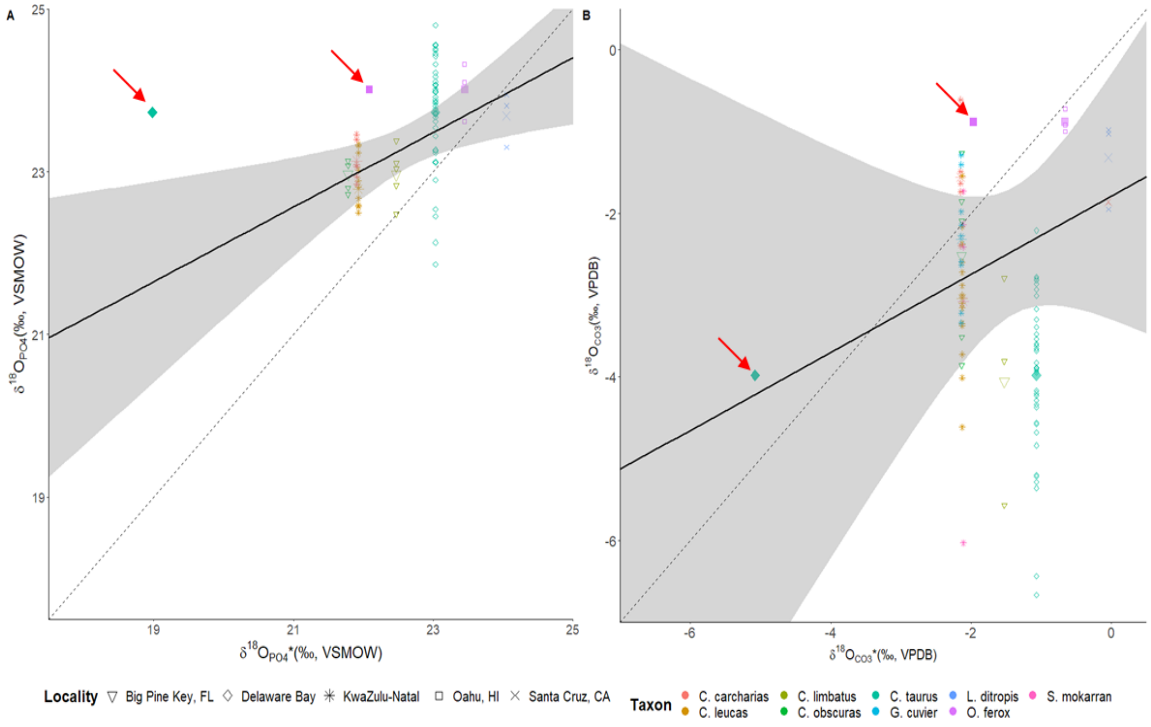

Figure 3. Empirical versus predicted values of phosphate and carbonate oxygen. Larger points are the averaged empirical and predicted values of localities and taxa. Smaller points are the data to show the variation. Red arrows indicate predicted values that use locality parameters, but were likely teeth not formed in the locality. Dashed line is to indicate a one-to-one ratio of predicted to empirical value. Black solid line is the linear regression, and the gray area is the confidence interval.

Table 4. Neogene $\delta^{18}O_{sw}$ and temperature probable estimations

Basin	Epoch	$\delta^{18}O_w$ mean (‰)	$\delta^{18}O_w$ SD (‰)	Temp (°C)	Temp SD	σ mean	σ SD
South Pacific	Miocene	-0.5	0.51	15.27	2.33	1.07	0.12
Central Pacific	Pliocene	-0.51	0.51	22.82	2.37	0.59	0.16
S. Central Atlantic	Miocene	-0.52	0.47	25.29	2.08	0.39	0.05
N. Central Atlantic	Pliocene	-1	0.39	28.1	1.79	1.73	0.45
N. Central Atlantic	Miocene	-0.51	0.49	24.28	2.17	0.8	0.07
East Pacific	Miocene	-0.48	0.51	15.33	3.44	1.38	0.92
West Atlantic	Pliocene	-0.51	0.49	12.26	2.5	0.92	0.24
West Atlantic	Miocene	-0.48	0.5	13.82	3.24	1.29	0.66
Paratethys	Miocene	-0.53	0.53	17.74	2.35	1.42	0.07

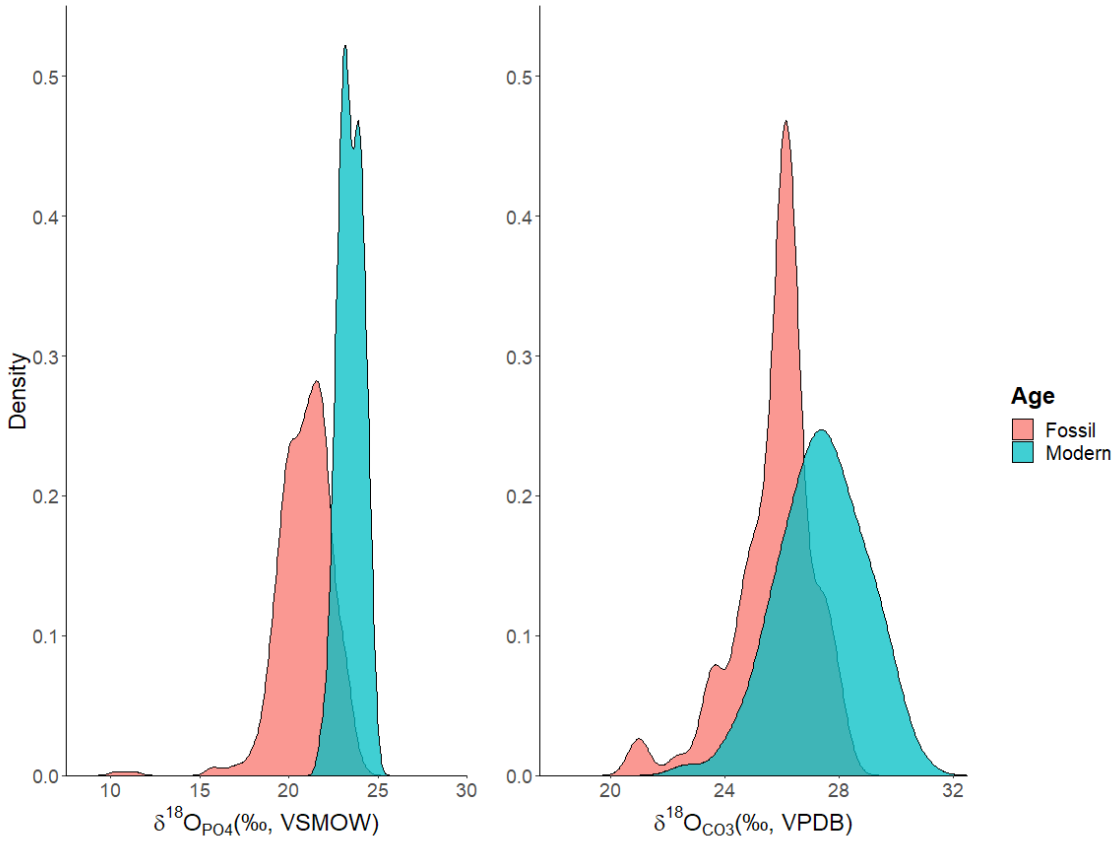

Figure 4. Distribution of all $\delta^{18}O$ values within phosphate and carbonate for modern and fossil teeth.

Fewer oxygen isotope studies have been conducted for the Pliocene using shark teeth, but our localities suggest that temperatures deviated from modern average temperatures. Central localities delineated after the Miocene, as the central Pacific averaged 22.6 ± 2.3°C and the central averaged 28.1 ± 1.5°C. Considering that extant sharks rarely swim above, much less survive, such temperatures (Grady et al., 2019), we exclude temperature estimations above 30°C. For the mid-latitude Atlantic locality, temperatures averaged 12.3 ± 2.5°C. We make no estimations for the Paratethys due to there being no $\delta^{18}O_{PO4}$ values from the locality in the literature, but Villafaña et al. (2020) and references therein reports of fossilized teeth found in the locality during the Pliocene.

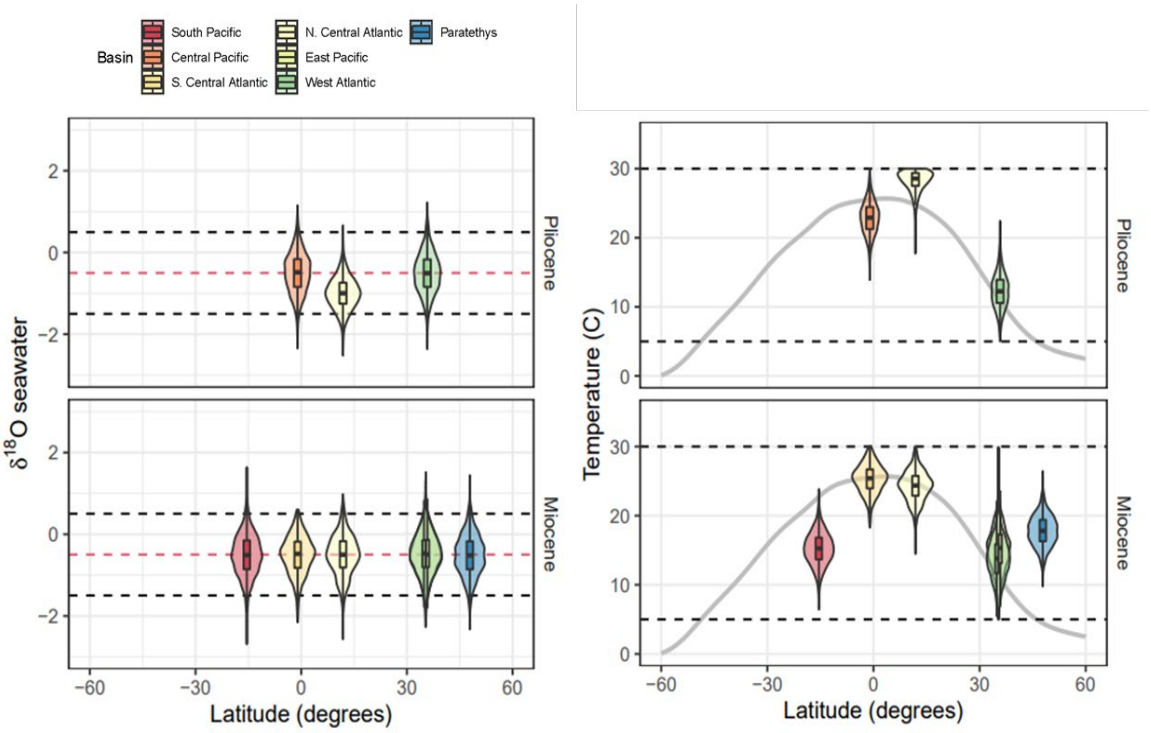

Figure 4. Average latitudinal temperature and $\delta^{18}O_{sw}$ gradient of basin localities during the Neogene. Solid gray line is contemporary average temperatures. Dashed black line for $\delta^{18}O_{sw}$ is the variability. Dashed black line for temperature is the range extant sharks can inhabit.

4. DISCUSSION

Our models, when compared to our empirical data, support that the oxygen isotope composition of phosphate from shark teeth is a reliable recorder of ambient sea temperature and $\delta^{18}O_{sw}$. First, the modern linear regression model demonstrates that $\delta^{18}O_{PO4}$ values from modern shark teeth are recording marine conditions where the teeth developed, not necessarily where teeth were collected. Localities with unusual variation of $\delta^{18}O_{PO4}$ values and uncharacteristic values likely suggest teeth developed before and/or during migration. On the other hand, the oxygen isotope composition of carbonate from shark teeth is either out of equilibrium or recording an additional factor that has not been accounted for. Second, we noticed similar ‘patterns’ when comparing

modern to fossilized $\delta^{18}O_{PO4}$ and $\delta^{18}O_{CO3}$ values. This would indicate that 1) post-extraction and -burial alteration likely did not occur, 2) the range and distribution of values shows regional and local environment characteristics during teeth formation, whereas variation reflects the fidelity of $\delta^{18}O_{PO4}$ and $\delta^{18}O_{CO3}$ values, and 3) the difference in marine conditions during the Neogene and present-day. Third, the Bayesian regression model estimates probable Neogene sea temperatures and $\delta^{18}O_{sw}$ values using $\delta^{18}O_{PO4}$ from fossilized teeth and prior knowledge of shark temperature habitat preferences, and a lower $\delta^{18}O_{sw}$ value likely reflects an influx of ^{16}O from high latitude precipitation. Our Bayesian results reflect oceanographic changes that occurred during Miocene – Pliocene transition and are supported by other proxies from these basins.

4.1 Modeling $\delta^{18}O_{PO4}$ and $\delta^{18}O_{CO3}$ Values

We compared predicted $\delta^{18}O^*$ teeth values to empirical $\delta^{18}O$ teeth values to assess how well modern shark teeth are recording marine conditions in their oxygen isotope composition. Addressing the fidelity $\delta^{18}O$ in modern shark teeth is important, as the mineral component of $\delta^{18}O$ from fossilized shark is the only measurable parameter for the Neogene.

Our models, when compared to our empirical data, support that the oxygen isotope composition of phosphate from shark teeth is a reliable recorder of ambient sea temperature and $\delta^{18}O_{sw}$ values. First, the modern linear regression model demonstrates that $\delta^{18}O_{PO4}$ values from modern shark teeth are recording marine conditions where the teeth developed, not necessarily where teeth were collected. Localities with unusual variation of $\delta^{18}O_{PO4}$ values and uncharacteristic values likely suggest teeth developed before and/or during migration. On the other hand, the oxygen isotope composition of carbonate from shark teeth is either out of equilibrium or recording an additional factor that has not been accounted for. Second, we noticed similar ‘patterns’ when comparing modern to fossilized $\delta^{18}O_{PO4}$ and $\delta^{18}O_{CO3}$ values, which indicates that 1) post-extraction and -burial alteration likely did not occur; 2) the range and distribution of values shows regional and local environment characteristics during teeth formation, whereas variation reflects the fidelity of $\delta^{18}O_{PO4}$ and $\delta^{18}O_{CO3}$ values; and 3) the difference in marine conditions during the Neogene and present-day. Third, the Bayesian regression model estimates probable Neogene sea temperatures and $\delta^{18}O_{sw}$ values using $\delta^{18}O_{PO4}$ from fossilized teeth and prior knowledge of shark temperature habitat preferences, and a lower $\delta^{18}O_{sw}$ value likely reflects an influx of ^{16}O from high latitude precipitation. Our Bayesian results reflect oceanographic changes that occurred during Miocene – Pliocene transition and are supported by other proxies from these basins.

4.1.1 Predicting Calcite $\delta^{18}O^*_{CO3}$ Values

The calcite equation from O’Neil et al. (1969) is still widely used for paleothermometry although we did consider using the carbonate-hydroxyapatite (CO_3-HAP) equation by Lécuyer et al. (2010). The authors note that 1) lab synthesized CO_3-HAP contains less carbonate and collagen than biogenic apatite (Daculsi et al., 1997; LeGeros et al., 1967), 2) concentrated [CO_3^{2-}] solutions mineralize out of equilibrium, resulting in 2-3‰

difference in fractionation (Kim & O'Neil, 1997), and 3) the inverse relation between oxygen isotope composition and temperature is not apparent for the equation. Hydroxyapatite is the also primary component of shark dentine and mammalian teeth, the latter which has a strong $\delta^{18}O_{CO3}$-$\delta^{18}O_{PO4}$ relationship that is not seen in marine ectotherms (Lécuyer et al., 2010 and references therein).

The offset between predicted and empirical $\delta^{18}O$ values was inconsistent and as high as 2.9‰, underestimating water temperatures by ~13°C at maximum. As shown by our comparison of predicted ($\delta^{18}O^*_{CO3}$) and empirical $\delta^{18}O_{CO3}$ values, the carbonate oxygen isotope composition from enameloid is not a reliable recorder of environmental conditions.

One explanation is that $\delta^{18}O_{CO3}$ is not formed in equilibrium, as $\delta^{18}O_{CO3}$ averages of taxa from the same locality are different compared to $\delta^{18}O_{PO4}$ means, which are nearly identical (**Table 1**). In Florida (USA), *C. limbatus* has an average of -4.1 ± 1.4‰ while the average for *C. obscuras* is -2.5 ± 1.1‰. In KwaZulu-Natal (South Africa), the $\delta^{18}O_{CO3}$ values differ by as much as 1.4‰ between taxa. Monterey Bay, CA (USA) had the lowest $\delta^{18}O_{CO3}$ difference of between taxa (0.6‰). On the other hand, $\delta^{18}O_{PO4}$ values are generally well constrained for taxa in these localities, which is expected since individuals share similar environmental conditions. It is possible that contamination of dentin may have occurred, but then there should be similar offsets in mean $\delta^{18}O_{PO4}$ values and deviation. Post-shedding diagenesis is highly unlikely as teeth are from extant sharks and were extracted. Karnes (2022) proposed an influence of environmental, metabolic, and diet (DIC) in fluorapatite as a vital effect, resulting in $\delta^{18}O_{CO3}$ variation in sharks, which has also been previously noted (Lécuyer et al., 2010; Vennemann et al., 2001). We do not go into the oxygen isotope dynamics of diet and metabolism, as this study is focused on environmental influences of $\delta^{18}O$ values; however, Spero et al. (1997) discovered the inverse relationship between [CO_3^{2-}] and $\delta^{18}O_{CO3}$ (and $\delta^{13}C_{CO3}$) from aquarium reared *Orbulina universa*. Zeebe (1999) proposed that oxygen isotope composition of the sum of DIC decreases with pH in foraminifera, which might explain the vital effect seen in other biogenic carbonates such as CO_3 in apatite, as suggested by (Lécuyer et al., 2010).

Modern empirical $\delta^{18}O_{CO3}$ and offset $\delta^{18}O^*_{CO3}$ values also suggest an environmental influence of pH, based on taxa and their vertical and/or horizontal movement. Seawater pH decreases with increasing depth and latitude, therefore [CO_3^{2-}] increases with increasing temperatures at the surface and lower latitudes (Feely et al., 2004, 2008, 2009; Figuerola et al., 2021; Jiang et al., 2015; Wu et al., 2019). If fractionation of $^{18}O/^{16}O$ within enameloid carbonate is similar to the tests of *O. universa*, then we expect sharks swimming in less alkaline waters to have greater $\delta^{18}O_{CO3}$ values. Compared to pelagic ectothermic species, benthopelagic ectothermic species (*O. ferox* and *G. cuvier*) move vertically along the seafloor and had higher $\delta^{18}O_{CO3}$ values with less variation and a $\delta^{18}O^*_{CO3}$ offset of 0.2‰ compared to ectothermic pelagic species. Specifically, *O. ferox* had the highest $\delta^{18}O_{CO3}$ values with the least variation, possibly because it is relatively sedentary, eating demersal prey at depth and not swimming vertically through the water column (Fergusson et al., 2008). Similarly, *G. cuvier* had the second highest $\delta^{18}O_{CO3}$ value and is a more active species, swimming to the surface and to brackish waters to

hunt. Traversing through waters with different chemical species of DIC and alkalinities may explain the higher variation for *G. cuvier*. The remaining ectothermic species are pelagic, with lower $\delta^{18}O_{CO3}$ values, which may be indicative of warmer surface temperatures, higher pH, and less acidic chemical species of DIC. This hypothesis is supported by the taxa from Florida and KwaZulu-Natal. In Florida, *C. limbatus* swims relatively close to the surface compared to *C. obscuras*, which resides at greater depths (Tinari & Hammerschlag, 2021). Therefore, *C. limbatus* has lower $\delta^{18}O_{CO3}$ values, whereas *C. obscuras* had higher $\delta^{18}O_{CO3}$ values for the same locality. Compared to *G. cuvier*, *C. leucas* and *S. mokarran* swim closer to the surface (Tinari & Hammerschlag, 2021) and had similarly low $\delta^{18}O_{CO3}$ values. Mesothermic species have interesting values of $\delta^{18}O_{CO3}$, being consistently around ~1.5 – 2‰, regardless of latitude. This $\delta^{18}O_{CO3}$ range may be due to mesotherms ability to generate heat, allowing them to swim into colder waters in higher latitudes, in the open ocean, and at depth (see **§4.1.5** for more discussion about mesotherms). Future use of $\delta^{18}O_{CO3}$ as a paleothermometer should probable be reserved until the mechanics of oxygen fractionation in carbonate in shark teeth is resolved.

4.1.2 Predicting Fluorapatite $\delta^{18}O^*_{PO4}$

We reviewed several generated linear regressions for the phosphate oxygen prediction model. Equations considered were Lécuyer et al. (2013), Pucéat et al. (2010), Longinelli & Nuti (1973), and Kolodny et al. (1983). Lécuyer et al. (2013) combined linglulids with 1 extant shark tooth and 5 specimens from hybodontiformes, an extinct group of elasmobranchs. Pucéat et al. (2010), who reared seabreams in aquarium water that had inconsistent oxygen isotope composition. Longinelli & Nuti (1973), who pioneered the use of fish teeth for thermometry, but mixed dentin, pulp, and bones in measurements Finally, Kolodny et al. (1983) used the whole tooth like Longinelli & Nuti (1973), but included both freshwater and marine fish, and was rescaled by Lécuyer et al. (2013) to reflect the new NBS120b $\delta^{18}O_{PO4}$ value of 21.4‰ rather than 20.0‰. The Kolodny et al. (1983) equation was used as a comparison of fluorapatite oxygen-phosphate to calcite oxygen-carbonate fractionating at equilibrium.

Predictions were linear within 1.0‰ of empirical values with some modest and anomalous exceptions. Some $\delta^{18}O^*_{PO4}$ predictions had a modest offset of 1.2‰. For example, this offset in *C. obscuras* could be due to either migrating to high latitudes in the winter or residing at greater depths in the water column (Hoffmayer et al., 2014; Tinari & Hammerschlag, 2021). Using the empirical $\delta^{18}O_{PO4}$ value, a temperature estimate of ~24.5℃ provides a better $\delta^{18}O^*_{PO4}$ value, which is more aligned with temperatures recorded at depth from shark tagging studies (Kroetz et al., 2021) than the mean seasonal SST value used for the initial prediction. This discrepancy in $\delta^{18}O^*_{PO4}$ values indicates that teeth reflect the preferred depth rather than near sea surface waters. Another possibility is that the teeth were extracted from a population of *O. obscuras* residing in Florida the same time as *C. limbatus*, given they had the same empirical $\delta^{18}O_{PO4}$ mean. In contrast, *C. carcharias* also had an offset of 1.2‰; the empirical value of 23.1‰ estimates a temperature of ~19.1℃, which agrees with SST for sharks caught in Richard's Bay and Michael's-on-Sea of South Africa (Cliff et al., 1989).

It is possible that prediction parameters were not accurate for this locality, as direct buoy SST data were unavailable for South Africa.

4.1.3 Migration, mayhaps

The teeth of *C. taurus* and *O. ferox* (both sand tiger sharks) were likely recording water conditions different than their caught locality. The anomalous $\delta^{18}O^*_{PO4}$ values were well above empirical $\delta^{18}O_{PO4}$ values by < 5‰. A migratory shark can form a tooth in one location and shed or use it elsewhere (i.e., have it in the function 1 or 2 position). Shark teeth are regularly shed and replaced, although the rate of development and loss is poorly known for most species. A migration signal has been hinted at in previous studies (Aguilera et al., 2017; Amiot et al., 2008; Barrick & Fischer, 1993; Fischer et al., 2013; Kim et al., 2020; Kocsis et al., 2007; Pellegrini & Longinelli, 2008; Roelofs et al., 2017) and is an explanation for these $\delta^{18}O_{PO4}$ and $\delta^{18}O^*_{PO4}$ offset values in *C. taurus* and *O. ferox*.

The modern model produced an approximate mean $\delta^{18}O^*_{PO4}$ value of 19.0 ± 0.7‰ using average SST and $\delta^{18}O_{sw}$ values during the months *C. taurus* remain in Delaware Bay. These parameters would suggest that teeth formed in brackish waters, as the alternative suggests warmer waters. While this prediction is agreeable for Delaware Bay, the average empirical value suggests teeth did not develop there. A study by Teter et al. (2015) reports that tagged *C. taurus* from Delaware Bay migrate to North Carolina and Florida in winter months. The region between Florida and North Carolina is likely represented by $\delta^{18}O_{PO4}$ values between 21 – 23‰, as these lower values would indicate warmer temperatures. The average empirical $\delta^{18}O_{PO4}$ value of 23.7‰ and general range between 23 - 25‰ (**Fig 1**) of *C. taurus* support those teeth likely formed somewhere within the region of Delaware Bay and North Carolina. We made a second prediction considering migration and used North Carolina marine conditions. Seawater conditions from North Carolina predict a value of 23.0 ± 0.5‰ $\delta^{18}O^*_{PO4}$, which suggest that the locality is more representative of the empirical value.

While the migrations of *C. taurus* in the USA have been well studied, *O. ferox* remains more elusive. This species is benthopelagic and prefers deeper, colder waters. In the Pacific Ocean, *O. ferox* will swim at depths of ~185 – 310m in temperatures between 9-18°C (Clarke, 1972; Fergusson et al., 2008). It is also suspected to migrate latitudinally at depth (Fergusson et al., 2008). Using surface water temperature conditions produced a predicted average value of 22.6‰, whereas the empirical average value was 24.0 ± 0.4‰. We adjusted the model temperature value to a colder average at depth based on data from Fishbase (2022), which resulted in $\delta^{18}O^*_{PO4}$ = 23.5‰. Although this temperature average is below the minimum monthly mean SST of Oahu, HI, it better aligns with the empirical value that likely reflects temperatures at depth.

4.1.4 Migration, Mesothermy, and Metabolism

A handful of extant sharks within the *Lamnidae* family, and potentially a few of the *Alopiidae* family, are mesotherms, meaning that they temporarily elevate their body temperature. Mesothermic species are *C. carcharias*, *Isurus oxyrinchus*, *Isurus paucus, Lamna nasus,* and *Lamna ditropis* (Dickson & Graham, 2004 and references therein),

and possibly thresher sharks *Alopias pelagius*, *Alopias superciliosus*, and *Alopias vulpinus* (Bernal et al., 2012; Dickson & Graham, 2004). The duration of elevated temperature and effects on body water is not completely understood so we include mesothermic sharks in our analysis.

Mesothermic species (*L. ditropis* and *C. carcharias* in our dataset) may be recording elevated body temperatures within the phosphate oxygen isotopic composition of their teeth, but inference is inconclusive given our limited modern dataset. Mesotherms can migrate to the open ocean and high latitudes by temporarily elevating body temperature (Grady et al., 2019). Depending on the species, generation of heat can occur either through digestion or increase use of red muscle tissue for hunting (Bernal et al., 2012). In Kwazulu-Natal, *C. leucas* and *C. carcharias* $\delta^{18}O_{PO4}$ values overlap and the mean $\delta^{18}O_{PO4}$ value of *C. carcharias* indicates a colder body temperature. Further, *L. ditropis* has the same mean $\delta^{18}O_{PO4}$ value as *C. taurus* from Delaware Bay, a similar latitude. We would expect lower $\delta^{18}O_{PO4}$ value if teeth are recording elevated body temperatures, and greater variation since generation of body temperature is temporary. If there is a metabolic signal, the true $\delta^{18}O_{PO4}$ value may be influenced by ambient water temperatures.

4.1.5 Comparing $\delta^{18}O^*_{PO4}$ and $\delta^{18}O^*_{CO3}$ Prediction Models

The Kolodny et al. (1983) equation (**Eqn 1**) generally predicts $\delta^{18}O^*_{PO4}$ greater than the empirical value, while the O'Neil et al. (1969) equation generally predicts $\delta^{18}O^*_{CO3}$ lower than the empirical value. Model $\delta^{18}O^*_{PO4}$ values have more coherence with empirical $\delta^{18}O_{PO4}$ values when utilizing species and locality specific habitat temperature preferences. This temperature adjustment shifts $\delta^{18}O^*_{CO3}$ for Delaware Bay outside the confidence interval but puts Hawaii near the one-to-one line.

Apart from Hawaii, our $\delta^{18}O^*_{PO4}$-$\delta^{18}O_{PO4}$ shows a latitude gradient, with lower latitude (warmer) localities having lower oxygen isotope composition while higher latitude (colder) localities have a ^{18}O-enriched composition. This gradient is not apparent with $\delta^{18}O^*_{CO3}$-$\delta^{18}O_{CO3}$. This further supports that oxygen isotope composition from phosphate is a reliable recorder of ambient marine conditions when considering shark species ecology, whereas the oxygen isotope composition of carbonate is more complicated.

Interestingly, localities that have large $\delta^{18}O^*_{PO4}$-$\delta^{18}O_{PO4}$ offsets (Delaware Bay and Hawaii), prior to temperature adjustments, have $\delta^{18}O^*_{CO3}$ overpredictions offset by ~1.0‰ to empirical $\delta^{18}O_{CO3}$ values. This $\delta^{18}O^*_{CO3}$-$\delta^{18}O_{CO3}$ offset may be reflective of the concentration of phosphate to alkalinity, as the concentration of phosphate as a proxy for DIC with correlation in phosphate and alkalinity (Wu et al., 2019).

4.2 Climate Patterns in Fossil & Modern Teeth

Fossil and modern teeth have similar range and variation of $\delta^{18}O_{CO3}$ and $\delta^{18}O_{PO4}$, albeit fossil teeth values are ^{18}O-depleted. The $\delta^{18}O$ offset for phosphate was ~2.0‰ and for carbonate was ~2.7‰. We interpret these $\delta^{18}O$ average values offsets as difference between the Neogene and Modern climate. Modern seawater salinity is well-mixed, with an average $\delta^{18}O_{sw}$ value 0.0 ± 0.5‰ (Craig & Gordon, 1965). For the Neogene, the

average global oxygen isotope composition of seawater is approximated to be -0.5‰ (Billups, 2002; Lear et al., 2000) as a result from polar ice cap melt. This lower $\delta^{18}O$ value contributes to lower $\delta^{18}O_{PO4}$ values from fossil shark teeth, as there is small overlap between fossil and modern values. There is significant overlap of fossil and modern $\delta^{18}O_{CO3}$ values, which perhaps supports the unknown factor causing relatively large variation in $\delta^{18}O_{CO3}$. Modes of lower, but prominent density of carbonate and phosphate of modern and fossil teeth values may be due to the spatial distribution of data. Localities from fossil teeth were from Pacific and Atlantic coasts ranging the low latitudes (15° S) of South America to mid latitudes (~35° N) of North America and the isolated Paratethys Sea (~46 - 50° N), whereas modern teeth spanned off the Pacific and Atlantic Shorelines of North America (~21 – 39° N) and off the Indian shoreline in South Africa (28.5° S).

The range of phosphate, and perhaps carbonate, $\delta^{18}O$ values is a result of salinity tolerance in some shark species. Taxa with $\delta^{18}O_{PO4}$ values considered to have an influx of freshwater were *†C. cuspidata*, *C. leucas, †C. chubutensis* and *†N. eurybathrodon*, all from the North Central Atlantic and Paratethys (Domingo Carrillo-Bricenõ et al., 2019; Kocsis et al., 2007). The only extant shark known to enter freshwater is *C. leucas* (Voigt and Weber 2011), whereas *†C. cuspidata* was likely capable of lower salinity waters like a possible extinct relative *†S. macrota* (Kim et al., 2020). *In addition, †N. eurybathrodon teeth are often found with other specimens from euryhaline species (C. leucas, N. brevirostris)* (Domingo Carrillo-Bricenõ et al., 2019). *In contrast, †C. chubutensis is related and co-occuring with †C. megalodon, which have not been reported to swim in hyposaline waters.* However, Domingo Carrillo-Bricenõ et al. (2019) proposed that *†C. chubutensis* may have also been a euryhaline species. We expand on paleoenvironmental interpretations of $\delta^{18}O_{PO4}$ values in the next section, as mineralized $\delta^{18}O$ is largely affected by salinity and geography (Zachos et al., 2001).

4.3 Estimating Probable Neogene Temperatures and $\delta^{18}O_{sw}$

4.3.1 Bayesian Regression Model Description

We developed a Bayesian regression model to estimate probable sea temperatures and $\delta^{18}O$ of seawater. We utilized measured $\delta^{18}O_{PO4}$ values from Neogene shark teeth supplemented by $\delta^{18}O_{PO4}$ values from previous studies and used the relationship from Kolodny et al. (1983; **Eqn 1**,**Table 4**). While there have been studies (a few of which we have included in the metadata) that measure $\delta^{18}O_{CO3}$ from Neogene-aged shark teeth, we exclude the oxygen isotope composition of carbonate based on our results from **§4.1.2**.

Shark teeth record low resolution trends of marine conditions in the nearshore; however, the spatiotemporal abundance of teeth metadata allows the model to produce a Neogene latitudinal temperature gradient. Understanding oceanography and ecology is important to elucidate latitudinal thermal gradients. Here, we use our knowledge of shark ecology and oceanographic events, corroborated with proxies by other studies, to interpret the generated latitude temperature gradient for the Neogene.

4.3.2 Miocene

Our model suggests the Miocene thermohaline circulation was similar to modern, as temperatures follow a general latitudinal gradient much like today, and that global $\delta^{18}O_{sw}$ values were slightly lower than 0‰. Our model indicates the Central Atlantic (Brazil and Caribbean localities) temperature averages are essentially the same as contemporaneous temperatures from these latitudes. Why did our shark teeth produce Miocene temperature estimates similar to present-day? The Isthmus of Panama likely had not yet bridged Central and South America, providing access between the Pacific and Atlantic Oceans. However, the dating of the closure during the Neogene is still highly contested (see Bacon et al. [2015]; Montes et al. [2015]; O'Dea et al., [2016] and related comments and replies). We do not attempt to establish the seaway closure (or other gateways) here because of the low resolution of temperature and absolute time provided by fossil shark teeth. It is possible that, given the global shift in currents during the Neogene as a result of gateway closures and openings (Steinthorsdottir et al., 2021), and consequential changes in marine chemistry differed between the oceans (O'Dea et al., 2016; Preiss-Daimler et al., 2021), shark species may simply have affinities for marine conditions (Tinari & Hammerschlag, 2021). This affinity might explain why the taxa became almost exclusively euryhaline in the N. Central Atlantic basin during the Pliocene (**§4.3.3;** Domingo Carrillo-Bricenõ et al., 2019), as the basin became inhabitable for most shark species.

The West Atlantic (North and South Carolina, USA) and East Pacific (California, USA) basins had similar temperature averages, with the East Pacific being slightly elevated compared to the West Atlantic. Deep-sea Pacific and Atlantic foraminifera $\delta^{18}O_{CO3}$ records agree that the Pacific Ocean was warmer during the Miocene (Westerhold et al., 2020; Zachos et al., 2001). It's also possible that these Pacific sharks, like their modern relatives, migrated from warm waters in Hawaii, Baja California (Mexico) (Weng et al., 2007), or Australia (Jorgensen et al., 2010), all of which are situated between equatorial to upper low latitudes. It's also possible that West Atlantic taxa migrated from colder water in higher latitudes. Since our West Atlantic and East Pacific dataset is a mixture of mesotherms and ectotherms with different migration patterns, the temperature estimations may be averages representing the overall conditions of these two oceans, which is still supported by the foraminifera record mentioned earlier. We would like to note that during the Miocene-Pliocene transition, *†C. hastalis* co-occurred and had a similar trophic level to *C. carcharias* (McCormack et al., 2022). The occurrence of these two shark teeth in the bone beds of the Temblor Fm. in our dataset is intriguing, as the formation is dated to Early Miocene and *C. carcharias* is considered to have emerged in the Late Miocene. Future studies should consider that 1) the dating of the Temblor Fm. needs to be further evaluated or 2) *C. carcharias* may have diverged earlier from *†C. hastalis*.

The South Pacific (Peru) estimated mean temperature was substantially colder than modern temperatures at low latitude. The range of estimated temperature from our model agrees with modern monthly SST averages (NOAA, 1971). While Amiot et al. (2008) compared $\delta^{18}O_{PO4}$ values to benthic foraminifera $\delta^{18}O_{CO3}$ records and found that

shark teeth followed Miocene temperature trends, we adjusted the age of teeth from Amiot et al. (2008) and (Kim, 2011) to be older based on strontium isotopes and zircon dating of shark teeth by Ehret et al. (2012). This recalibration shifts teeth to only the Miocene epoch and better fits the Pacific foraminifera record. As mentioned by Amiot et al. (2008), the Humboldt Current diverges from the Antarctic Circumpolar Current, which may have initiated after the opening of the Drake Passage and Tasmanian Gateway (Scher & Martin, 2006). The Humboldt Current pushes deep water along the Peruvian coasts, which explains the lower paleotemperature estimates from our Bayesian model and similarity to modern temperatures (**Fig 5**).

Finally, Paratethys waters were estimated to be much warmer than modern SST averages at this latitude. Paratethys had gateway access to the Atlantic and Indian Oceans, and limited access to the Tethys Sea from orogenic formation (Vennemann & Hegner, 1998; Zachos et al., 2001). This deviation at latitude can be potentially explained by its influence from both freshwater and marine waters. Two teeth had oxygen and strontium isotopic compositions that highly suggest orogenic water origination (Kocsis et al., 2007), as teeth were found in what was once small, shallow seaway near alpine delta fans (Berger et al., 2005). Kocsis et al. (2007) concluded that it was unlikely diagenesis altered only oxygen and strontium isotope composition, because rare earth element (REE) patterns were similar across all teeth in the dataset of the original study. Additionally, Nd isotope measurements corroborate orogenic sea water (Kocsis et al., 2009), however Nd isotope values indicate that the Paratethys was largely sourced from the Indian Ocean in the early Miocene, then the Atlantic Ocean in the middle Miocene (Vennemann & Hegner, 1998). A hypersaline environment could also produce temperature estimations higher than averages found at the same latitude today, however the model $\delta^{18}O_{sw}$ value supports that water was of marine origin. The oxygen isotope composition from these two teeth may be skewing estimations towards warmer temperatures, considering their extremely low $\delta^{18}O_{PO4}$ values (10.3 ‰ and 11.3‰). A combination of warm temperatures compounded by gateway closure, due to tectonic uplift, likely assisted in the eventual desiccation of the Paratethys (Palcu et al., 2021).

4.3.3 Pliocene

The number of Pliocene basins represented in the literature from fossil shark teeth oxygen isotope composition were reduced to half. Temperature and $\delta^{18}O_{sw}$ estimates deviate from modern averages, despite the Pliocene continental formations being in their modern positions and modern climate conditions best resembling the epoch (Burke et al., 2018), but follow general latitudinal temperature trends that occurred in the Atlantic and Pacific during the Piacenzian (Karas et al., 2017).

A cooling in mid-latitude West Atlantic and tropical South Pacific as well as warming in North Central Atlantic is estimated based on our model results. West Atlantic shark teeth are from the Yorktown Formation, a horizon that experienced warming during the mid-Pliocene Warm Period. The estimated temperature average from our Bayesian model indicates that teeth formed in much colder water compared to other Yorktown Fm. SST proxies (i.e., $U_{37}^{k'}$ and $\delta^{18}O_{CO3}$ from mollusks; (Dowsett et al., 2021; Winkelstern et al.,

2013). It is possible that either these shark teeth developed at depth as temperature estimates corroborate benthic (20 to ≥ 100m) mollusk estimates (Johnson et al., 2016), or at higher mid latitudes based on planktic foraminifera SST (Karas et al., 2017) and migrated to the West Atlantic basin locality. We lean towards the latter, considering our West Atlantic fossilized assemblage has 1) present-day species and modern analogues that are highly migratory (for example, *C. carcharias* (Curtis et al., 2014; Skomal et al., 2017), *C. taurus* (Kneebone et al., 2014; Teter et al., 2015)*, I. oxyrinchus* (Casey & Kohler, 1992; Compagno, 2001)), and 2) has preserved remains of relatives that are globally distributed (Cione et al., 2012; Kim et al., 2020; Pimiento et al., 2016).

Indeed, the temperature estimates show an increased interhemispheric temperature gradient, as the mid-latitude West Atlantic cooled while the North Central Atlantic basin supposedly experienced a ~4°C increase. Our model suggests decreasing $\delta^{18}O_{sw}$ values and supports the interpretation by (Domingo Carrillo-Bricenõ et al., 2019) of lower salinity waters, as overall taxa was reduced to euryhaline species with relatively low $\delta^{18}O_{PO4}$ values indicating brackish waters. While our N. Central Atlantic basin had become a partially enclosed bay, the Caribbean generally experienced warming and increased salinity throughout the Pliocene, recording a relatively high $\delta^{18}O_{CO3}$ signal (Groeneveld et al., 2008; Gussone et al., 2004). Despite this significant difference in salinity, our temperature estimates corroborate with Caribbean SST from Mg/Ca of planktonic foraminifera and algae alkenones (Groeneveld et al., 2008; Gussone et al., 2004; Steph et al., 2010). Thus, the ^{18}O-enriched Caribbean is a result of increased evaporation and increased salinity (Steph et al., 2006, 2010), rather than enrichment based on just warm temperatures, after the closure of the Panamanian Gateway and subsequent decrease of Pacific seawater flow through the gateway. There is evidence of salinity and $\delta^{18}O_{CO3}$ decoupling in the central Pacific and Atlantic from deep sea multiproxies (O'Dea et al., 2016 and references therein), which is also supported by our model results.

Our paleotemperature estimates were generally several degrees lower than previous results in (Pellegrini & Longinelli, 2008), whose $\delta^{18}O_{PO4}$ values were part of the Central Pacific Basin dataset in this study. The original authors estimated paleotemperatures using a 'modern' $\delta^{18}O_{sw}$ value of 0.3‰ and a value of 1.2‰ to signify the 'difference' between interglacial and glacial ocean water, which substantially increased the estimates. The use of these $\delta^{18}O_{sw}$ values is interesting, as many recent studies on Miocene – Pliocene climate still use the modern well-mixed value of 0.0‰ because the unlikely scenario that it would be a completely ice-free climate. An ocean with relatively lower polar ice volume would have a lower $\delta^{18}O_{sw}$ value, similar to our model results and previous studies used here (e.g., Aguilera et al. 2017; Domingo Carrillo-Bricenõ et al. 2019). Our temperature estimates for the Central Pacific basin agree with coupled Mg/Ca – $\delta^{18}O_{CO3}$ temperature estimates from planktonic foraminifera and alkenone estimates (Steph et al., 2010). Additionally, (Pellegrini & Longinelli, 2008) used only shark teeth from *Carcharhinus sp.*, making interpretation of marine conditions and the likelihood that teeth formed off the coast of Ecuador difficult.

5. CONCLUSION

Present-day SST and $\delta^{18}O_{sw}$ values are used to model phosphate and carbonate $\delta^{18}O^*$ values within the enameloid of shark teeth for the epipelagic zone. The $\delta^{18}O^*_{PO4}$ predictions are more correlated and less variable than $\delta^{18}O^*_{CO3}$ when compared to empirical values. Empirical $\delta^{18}O_{PO4}$ average values appear to reflect a latitudinal gradient. However, knowledge of shark ecology should be thoroughly considered as demonstrated here.

Shark ecology, especially migration, should be considered when using shark teeth for environmental reconstruction. The use of teeth from highly migratory sharks should be reserved unless migration patterns have been well studied. Physiology is another biological factor to study as some sharks within the Lamindae family are mesothermic. However, mesothermy appears to have a negligible effect on $\delta^{18}O_{PO4}$ values, considering values are within ectothermic variation signifying that the ambient sea temperature influence is stronger. We look forward to the quantification of mesothermic shark body temperature, to not only improve models, but also as an additional temperature proxy for open oceans.

We see similar summary statistics for temperature and $\delta^{18}O_{SW}$ values between our modern and fossilized samples. The variation seen in our large dataset of extant and extinct sharks reflects the different temperatures and salinities shark species can inhabit. The offset between modern and fossilized shark teeth $\delta^{18}O$ values likely reflects the mixing conditions and polar ice volume difference between present-day and the Neogene.

The Neogene climate and geography is most relevant when compared to contemporary conditions and is used as a case study to interpret the paleo-oceanography and paleoclimate. Our Bayesian regression model uses $\delta^{18}O_{PO4}$ from fossilized teeth to estimate probability of temperature and $\delta^{18}O_{sw}$; estimates generally agree with other proxy interpretations of marine conditions. Anomalies can usually be explained by shark species migration habits and hyper- or hypo-salinity. Bayesian regression allows us to interpret based on probability of $\delta^{18}O_{PO4}$, temperature, and $\delta^{18}O_{sw}$, rather than just $\delta^{18}O_{PO4}$ values alone. As insights to shark paleoecology increase, environmental interpretations will provide important complementary context.

REFERENCES

Aguilera, O., Luz, Z., Carrillo-Briceño, J. D., Kocsis, L., Vennemann, T. W., De Toledo, P. M., et al. (2017). *Neogene sharks and rays from the Brazilian 'Blue Amazon.' PLoS ONE* (Vol. 12). https://doi.org/10.1371/journal.pone.0182740

Amiot, R., Göhlich, U. B., Lécuyer, C., de Muizon, C., Cappetta, H., Fourel, F., et al. (2008). Oxygen isotope compositions of phosphate from Middle Miocene-Early Pliocene marine vertebrates of Peru. *Palaeogeography, Palaeoclimatology, Palaeoecology*, *264*(1–2), 85–92. https://doi.org/10.1016/j.palaeo.2008.04.001

Bacon, C. D., Silvestro, D., Jaramillo, C., Smith, B. T., Chakrabarty, P., & Antonelli, A.

(2015). Biological evidence supports an early and complex emergence of the Isthmus of Panama. *Proceedings of the National Academy of Sciences of the United States of America*, *112*(19), 6110–6115. https://doi.org/10.1073/pnas.1423853112

Barrick, R. E., & Fischer, A. G. (1993). PALEOTEMPERATURES VERSUS SEA LEVEL: OXYGEN ISOTOPE SIGNAL FROM FISH BONE PHOSPHATE OF THE MIOCENE CALVERT CLIFFS, MARYLAND. *Paleoceanography*, *8*(6), 845–858.

Berger, J. P., Reichenbacher, B., Becker, D., Grimm, M., Grimm, K., Picot, L., et al. (2005). Paleogeography of the Upper Rhine Graben (URG) and the Swiss Molasse Basin (SMB) from Eocene to Pliocene. *International Journal of Earth Sciences*, *94*(4), 697–710. https://doi.org/10.1007/s00531-005-0475-2

Bernal, D., Carlson, J. K., Goldman, K. J., & Lowe, C. G. (2012). Energetics, Metabolism, and Endothermy in Sharks and Rays. *Biology of Sharks and Their Relatives*, 227–254. https://doi.org/10.1201/b11867-15

Billups, K. (2002). Late Miocene through early Pliocene deep water circulation and climate change viewed from the sub-Antarctic South Atlantic. *Palaeogeography, Palaeoclimatology, Palaeoecology*, *185*(3–4), 287–307. https://doi.org/10.1016/S0031-0182(02)00340-1

Botella, H., Donoghue, P. C. J., & Martínez-Pérez, C. (2009). Enameloid microstructure in the oldest known chondrichthyan teeth. *Acta Zoologica*, *90*(SUPPL. 1), 103–108. https://doi.org/10.1111/j.1463-6395.2008.00337.x

Burke, K. D., Williams, J. W., Chandler, M. A., Haywood, A. M., Lunt, D. J., & Otto-Bliesner, B. L. (2018). Pliocene and Eocene provide best analogs for near-future climates. *Proceedings of the National Academy of Sciences of the United States of America*, *115*(52), 13288–13293. https://doi.org/10.1073/pnas.1809600115

Carlson, S. J. (1991). Skeletal Biomineralization: Patterns, Processes and Evolutionary Trends. *Skeletal Biomineralization: Patterns, Processes and Evolutionary Trends*, (January 1990). https://doi.org/10.1007/978-1-4899-5740-5

Casey, J. G., & Kohler, N. E. (1992). Tagging studies on the shortfin mako shark (Isurus oxyrinchus) in the western north atlantic. *Marine and Freshwater Research*, *43*(1), 45–60. https://doi.org/10.1071/MF9920045

Center, U. D. > N. D. B. (1971). Meteorological and oceanographic data collected from the National Data Buoy Center Coastal-Marine Automated Network (C-MAN) and moored (weather) buoys. Retrieved from https://www.ncei.noaa.gov/archive/accession/NDBC-CMANWx

Cione, A. L., Cabrera, D. A., & Barla, M. J. (2012). Oldest record of the Great White Shark (Lamnidae, Carcharodon; Miocene) in the Southern Atlantic. *Geobios*, *45*(2), 167–172. https://doi.org/10.1016/j.geobios.2011.06.002

Clarke, T. (1972). Collections and submarine observations of deep benthic fishes and decapod Crustacea in Hawaii. *Pacific Science*, *26*(3), 310–317.

Cliff, G., Dudley, S. F. J., & Davis, B. (1989). Sharks caught in the protective gill nets off natal, South Africa. 2. the great white shark carcharodon carcharias (linnaeus).

South African Journal of Marine Science, *8*(1), 131–144. https://doi.org/10.2989/02577618909504556

Compagno, L. J. V. (2001). *Sharks of the World*. *Sharks of the World* (Vol. 2). https://doi.org/10.2307/j.ctv1574pqp

Craig, H., & Gordon, A. (1965). Deuterium and oxygen 18 variations in the ocean and the marine atmospher. *Stable Isotopes in Oceanic Studies and Paleotemperatures*, 9–130.

Curtis, T. H., McCandless, C. T., Carlson, J. K., Skomal, G. B., Kohler, N. E., Natanson, L. J., et al. (2014). Seasonal distribution and historic trends in abundance of white sharks, Carcharodon carcharias, in the western North Atlantic ocean. *PLoS ONE*, *9*(6). https://doi.org/10.1371/journal.pone.0099240

Daculsi, G., Bouler, J. M., & Legeros, R. Z. (1997). Adaptive crystal formation in normal and pathological calcifications in synthetic calcium phosphate and related biomaterials. *International Review of Cytology*, *172*, 129–191. https://doi.org/10.1016/s0074-7696(08)62360-8

Dickson, K. A., & Graham, J. B. (2004). Evolution and consequences of endothermy in fishes. *Physiological and Biochemical Zoology*, *77*(6), 998–1018. https://doi.org/10.1086/423743

Domingo Carrillo-Bricenõ, J., Luz, Z., Hendy, A., Kocsis, L., Aguilera, O., & Vennemann, T. (2019). Neogene Caribbean elasmobranchs: Diversity, paleoecology and paleoenvironmental significance of the Cocinetas Basin assemblage (Guajira Peninsula, Colombia). *Biogeosciences*, *16*(1), 33–56. https://doi.org/10.5194/bg-16-33-2019

Dowsett, H. J., Robinson, M. M., Foley, K. M., & Herbert, T. D. (2021). The Yorktown Formation: Improved Stratigraphy, Chronology, and Paleoclimate Interpretations from the U.S. Mid-Atlantic Coastal Plain. *Geosciences (Switzerland)*, *11*(12). https://doi.org/10.3390/geosciences11120486

Ehret, D. J., Macfadden, B. J., Jones, D. S., Devries, T. J., Foster, D. A., & Salas-Gismondi, R. (2012). Origin of the white shark Carcharodon (Lamniformes: Lamnidae) based on recalibration of the Upper Neogene Pisco Formation of Peru. *Palaeontology*, *55*(6), 1139–1153. https://doi.org/10.1111/j.1475-4983.2012.01201.x

Enax, J., Prymak, O., Raabe, D., & Epple, M. (2012). Structure, composition, and mechanical properties of shark teeth. *Journal of Structural Biology*, *178*(3), 290–299. https://doi.org/10.1016/j.jsb.2012.03.012

Enax, J., Janus, A. M., Raabe, D., Epple, M., & Fabritius, H. O. (2014). Ultrastructural organization and micromechanical properties of shark tooth enameloid. *Acta Biomaterialia*, *10*(9), 3959–3968. https://doi.org/10.1016/j.actbio.2014.04.028

Feely, R. A., Sabine, C. L., Lee, K., Berelson, W., Kleypas, J., Fabry, V. J., & Millero, F. J. (2004). The CaCO 3 -CO 2 -H 2 O system in soils. *Journal of Agronomic Education*, *305*. https://doi.org/10.2134/jae1985.0003

Feely, R. A., Sabine, C. L., Hernandez-Ayon, J. M., Ianson, D., & Hales, B. (2008).

Evidence for upwelling of corrosive “acidified” water onto the continental shelf. *Science*, *320*(5882), 1490–1492. https://doi.org/10.1126/science.1155676

Feely, R. A., Orr, J., Fabry, V. J., Kleypas, J. A., Sabine, C. L., & Langdon, C. (2009). Present and future changes in seawater chemistry due to ocean acidification. *Geophysical Monograph Series*, *183*(Table 1), 175–188. https://doi.org/10.1029/2005GM000337

Fergusson, I. K., Graham, K. J., & Compagno, L. J. V. (2008). Distribution, abundance and biology of the smalltooth sandtiger shark Odontaspis ferox (Risso, 1810) (Lamniformes: Odontaspididae). *Environmental Biology of Fishes*, *81*(2), 207–228. https://doi.org/10.1007/s10641-007-9193-x

Figuerola, B., Hancock, A. M., Bax, N., Cummings, V. J., Downey, R., Griffiths, H. J., et al. (2021). A Review and Meta-Analysis of Potential Impacts of Ocean Acidification on Marine Calcifiers From the Southern Ocean. *Frontiers in Marine Science*, *8*(January). https://doi.org/10.3389/fmars.2021.584445

Fischer, J., Schneider, J. W., Voigt, S., Joachimski, M. M., Tichomirowa, M., Tütken, T., et al. (2013). Oxygen and strontium isotopes from fossil shark teeth: Environmental and ecological implications for Late Palaeozoic European basins. *Chemical Geology*, *342*, 44–62. https://doi.org/10.1016/j.chemgeo.2013.01.022

Froese, R., & Pauly, D. (2022). FishBase. Retrieved from www.fishbase.org

Grady, J. M., Maitner, B. S., Winter, A. S., Kaschner, K., Tittensor, D. P., Record, S., et al. (2019). Metabolic asymmetry and the global diversity ofmarine predators. *Science*, *366*(January). https://doi.org/10.1126/science.aat4220

Groeneveld, J., Nürnberg, D., Tiedemann, R., Reichart, G. J., Steph, S., Reuning, L., et al. (2008). Foraminiferal Mg/Ca increase in the Caribbean during the Pliocene: Western Atlantic Warm Pool formation, salinity influence, or diagenetic overprint? *Geochemistry, Geophysics, Geosystems*, *9*(1), 1–21. https://doi.org/10.1029/2006GC001564

Gussone, N., Eisenhauer, A., Tiedemann, R., Haug, G. H., Heuser, A., Bock, B., et al. (2004). Reconstruction of Caribbean Sea surface temperature and salinity fluctuations in response to the Pliocene closure of the Central American Gateway and radiative forcing, using δ44/40Ca, δ18O and Mg/Ca ratios. *Earth and Planetary Science Letters*, *227*(3–4), 201–214. https://doi.org/10.1016/j.epsl.2004.09.004

Haario, H., Saksman, E., & Tamminen, J. (2001). An adaptive Metropolis algorithm. *Bernoulli*, *7*(2), 223–242. https://doi.org/10.2307/3318737

Hammerschlag, N., Gallagher, A. J., & Lazarre, D. M. (2011). A review of shark satellite tagging studies. *Journal of Experimental Marine Biology and Ecology*, *398*(1–2), 1–8. https://doi.org/10.1016/j.jembe.2010.12.012

Hoffmayer, E. R., Franks, J. S., Driggers, W. B., McKinney, J. A., Hendon, J. M., & Quattro, J. M. (2014). Habitat, movements and environmental preferences of dusky sharks, Carcharhinus obscurus, in the northern Gulf of Mexico. *Marine Biology*, *161*(4), 911–924. https://doi.org/10.1007/s00227-014-2391-0

Holbourn, A., Kuhnt, W., Clemens, S., Prell, W., & Andersen, N. (2013). Middle to late

Miocene stepwise climate cooling: Evidence from a high-resolution deep water isotope curve spanning 8 million years. *Paleoceanography*, *28*(4), 688–699. https://doi.org/10.1002/2013PA002538

Jiang, L. Q., Feely, R. A., Carter, B. R., Greeley, D. J., Gledhill, D. K., & Arzayus, K. M. (2015). Climatological distribution of aragonite saturation state in the global oceans. *Global Biogeochemical Cycles*, *29*(10), 1656–1673. https://doi.org/10.1002/2015GB005198

Johnson, A., Andrew, L. A., Melanie, J., Hilary, J., & Bernd, R. (2016). ISOTOPIC TEMPERATURES FROM THE EARLY AND MID-PLIOCENE OF THE US MIDDLE ATLANTIC COASTAL PLAIN , AND THEIR IMPLICATIONS FOR THE CAUSE OF REGIONAL MARINE CLIMATE CHANGE ATLANTIC COASTAL PLAIN , AND THEIR IMPLICATIONS FOR THE CAUSE OF REGIONAL MARINE.

Jorgensen, S. J., Reeb, C. A., Chapple, T. K., Anderson, S., Perle, C., Van Sommeran, S. R., et al. (2010). Philopatry and migration of Pacific white sharks. *Proceedings of the Royal Society B: Biological Sciences*, *277*(1682), 679–688. https://doi.org/10.1098/rspb.2009.1155

Karas, C., Nürnberg, D., Bahr, A., Groeneveld, J., Herrle, J. O., Tiedemann, R., & Demenocal, P. B. (2017). Pliocene oceanic seaways and global climate. *Scientific Reports*, *7*(June 2016), 4–11. https://doi.org/10.1038/srep39842

Karnes, M. E. (2022). *Enigmatic Carbonate Isotope Values in Shark Teeth: Evidence for Environmental and Diet Controls No Title*. University of California Merced.

Keenan, S. W. (2016). From bone to fossil: A review of the diagenesis of bioapatite. *American Mineralogist*, *101*(9), 1943–1951. https://doi.org/10.2138/am-2016-5737

Kim, S. L. (2011). Ecology and evolution of Cosmopolitodus hastalis and Carcharodon carcharias. In *Society of Vertebrate Paleontology*.

Kim, S. L., Zeichner, S. S., Colman, A. S., Scher, H. D., Kriwet, J., Mörs, T., & Huber, M. (2020). Probing the Ecology and Climate of the Eocene Southern Ocean With Sand Tiger Sharks Striatolamia macrota. *Paleoceanography and Paleoclimatology*, *35*(12), 1–21. https://doi.org/10.1029/2020PA003997

Kim, S. T., & O'Neil, J. R. (1997). Equilibrium and nonequilibrium oxygen isotope effects in synthetic carbonates. *Geochimica et Cosmochimica Acta*, *61*(16), 3461–3475. https://doi.org/10.1016/S0016-7037(97)00169-5

Kneebone, J., Chisholm, J., & Skomal, G. (2014). Movement patterns of juvenile sand tigers (Carcharias taurus) along the east coast of the USA, 1149–1163. https://doi.org/10.1007/s00227-014-2407-9

Kocsis, L., Vennemann, T. W., & Fontignie, D. (2007). Migration of sharks into freshwater systems during the Miocene and implications for Alpine paleoelevation. *Geology*, *35*(5), 451–454. https://doi.org/10.1130/G23404A.1

Kocsis, L., Vennemann, T. W., Hegner, E., Fontignie, D., & Tütken, T. (2009). Constraints on Miocene oceanography and climate in the Western and Central Paratethys: O-, Sr-, and Nd-isotope compositions of marine fish and mammal remains. *Palaeogeography, Palaeoclimatology, Palaeoecology*, *271*(1–2), 117–129.

https://doi.org/10.1016/j.palaeo.2008.10.003

Kolodny, Y., Luz, B., & Navon, O. (1983). Oxygen isotope variations in phosphate of biogenic apatites, I. Fish bone apatite-rechecking the rules of the game. *Earth and Planetary Science Letters*, *64*(3), 398–404. https://doi.org/10.1016/0012-821X(83)90100-0

Kroetz, A. M., Gulak, S. J. B., & Carlson, J. K. (2021). Horizontal and vertical movements of immature dusky sharks Carcharhinus obscurus in relation to commercial longline fisheries in the western North Atlantic Ocean. *Animal Biotelemetry*, *9*(1), 1–12. https://doi.org/10.1186/s40317-021-00258-8

Lear, C. H., Elderfield, H., & Wilson, P. A. (2000). Cenozoic deep-sea temperatures and global ice volumes from Mg/Ca in benthic foraminiferal calcite. *Science*, *287*(5451), 269–272. https://doi.org/10.1126/science.287.5451.269

Lécuyer, C., Balter, V., Martineau, F., Fourel, F., Bernard, A., Amiot, R., et al. (2010). Oxygen isotope fractionation between apatite-bound carbonate and water determined from controlled experiments with synthetic apatites precipitated at 10-37 °C. *Geochimica et Cosmochimica Acta*, *74*(7), 2072–2081. https://doi.org/10.1016/j.gca.2009.12.024

Lécuyer, C., Amiot, R., Touzeau, A., & Trotter, J. (2013). Calibration of the phosphate δ18O thermometer with carbonate-water oxygen isotope fractionation equations. *Chemical Geology*, *347*, 217–226. https://doi.org/10.1016/j.chemgeo.2013.03.008

LeGeros, R. Z. (1990). Chemical and crystallographic events in the caries process. *Journal of Dental Research*, *69*(SPEC. ISS. FEB.), 567–574. https://doi.org/10.1177/00220345900690s113

LeGeros, R.Z. (1981). Apatites in Biological Systems. *Progress in Crystal Growth and Characterization*, *4*(1–2), 1–45. https://doi.org/https://doi.org/10.1016/0146-3535(81)90046-0

LeGeros, Racquel Z., Trautz, O. R., LeGeros, J. P., Klein, E., & Paul Shirra, W. (1967). Apatite crystallites: Effects of carbonate on morphology. *Science*, *155*(3768), 1409–1411. https://doi.org/10.1126/science.155.3768.1409

Leung, J. Y. S., Nagelkerken, I., Pistevos, J. C. A., Xie, Z., Zhang, S., & Connell, S. D. (2022). Shark teeth can resist ocean acidification. *Global Change Biology*, (June 2021), 1–10. https://doi.org/10.1111/gcb.16052

Longinelli, A., & Nuti, S. (1973). Oxygen isotope measurements of phosphate from fish teeth and bones. *Earth and Planetary Science Letters*, *20*(3), 337–340. https://doi.org/10.1016/0012-821X(73)90007-1

Lucifora, L., Garcia, V., & Worm, B. (2011). Global Diversity Hotspots and Conservation Priorities for Sharks. *PloS One*, *6*(5). https://doi.org/10.1371/journal.pone.0019356

McCormack, J., Griffiths, M. L., Kim, S. L., Shimada, K., Karnes, M., Maisch, H., et al. (2022). Trophic position of Otodus megalodon and great white sharks through time revealed by zinc isotopes. *Nature Communications*, *13*(1), 1–10. https://doi.org/10.1038/s41467-022-30528-9

Miake, Y., Aoba, T., Moreno, E. C., Shimoda, S., Prostak, K., & Suga, S. (1991). Ultrastructural studies on crystal growth of enameloid minerals in elasmobranch and teleost fish. *Calcified Tissue International*, *48*(3), 204–217. https://doi.org/10.1007/BF02570556

Miller, K. G., Browning, J. V., John Schmelz, W., Kopp, R. E., Mountain, G. S., & Wright, J. D. (2020). Cenozoic sea-level and cryospheric evolution from deep-sea geochemical and continental margin records. *Science Advances*, *6*(20). https://doi.org/10.1126/sciadv.aaz1346

Mine, A. H., Waldeck, A., Olack, G., Hoerner, M. E., Alex, S., & Colman, A. S. (2017). Microprecipitation and δ18O analysis of phosphate for paleoclimate and biogeochemistry research. *Chemical Geology*, *460*(April), 1–14. https://doi.org/10.1016/j.chemgeo.2017.03.032

Montes, C., Cardona, A., Jaramillo, C., Pardo, A., Silva, J. C., Valencia, V., et al. (2015). Middle Miocene closure of the Central American Seaway. *Science*, *348*(6231), 226–229. https://doi.org/10.1126/science.aaa2815

O'Dea, A., Lessios, H. A., Coates, A. G., Eytan, R. I., Restrepo-Moreno, S. A., Cione, A. L., et al. (2016). Formation of the Isthmus of Panama. *Science Advances*, *2*(8), 1–12. https://doi.org/10.1126/sciadv.1600883

O'Neil, J. R., Clayton, R. N., & Mayeda, T. K. (1969). Oxygen isotope fractionation in divalent metal carbonates. *The Journal of Chemical Physics*, *51*(12), 5547–5558. https://doi.org/10.1063/1.1671982

Palcu, D. V., Patina, I. S., Șandric, I., Lazarev, S., Vasiliev, I., Stoica, M., & Krijgsman, W. (2021). Late Miocene megalake regressions in Eurasia. *Scientific Reports*, *11*(1), 1–12. https://doi.org/10.1038/s41598-021-91001-z

Pearson, P. N. (2012). Oxygen Isotopes in Foraminifera: Overview and Historical Review. *The Paleontological Society Papers*, *18*, 1–38. https://doi.org/10.1017/s1089332600002539

Pellegrini, M., & Longinelli, A. (2008). Palaeoenvironmental conditions during the deposition of the Plio-Pleistocene sedimentary sequence of the Canoa Formation, central Ecuador: A stable isotope study. *Palaeogeography, Palaeoclimatology, Palaeoecology*, *266*(1–2), 119–128. https://doi.org/10.1016/j.palaeo.2008.03.017

Pimiento, C., MacFadden, B. J., Clements, C. F., Varela, S., Jaramillo, C., Velez-Juarbe, J., & Silliman, B. R. (2016). Geographical distribution patterns of Carcharocles megalodon over time reveal clues about extinction mechanisms. *Journal of Biogeography*, *43*(8), 1645–1655. https://doi.org/10.1111/jbi.12754

Posner, A. S., Blumenthal, N. C., & Betts, F. (1984). Chemistry and structure of precipitated hydroxyapatites. *Phosphate Minerals*, *10*, 330–350. https://doi.org/10.1007/978-3-642-61736-2_11

Preiss-Daimler, I., Zarkogiannis, S. D., Kontakiotis, G., Henrich, R., & Antonarakou, A. (2021). Paleoceanographic perturbations and the marine carbonate system during the middle to late miocene carbonate crash— a critical review. *Geosciences (Switzerland)*, *11*(2), 1–24. https://doi.org/10.3390/geosciences11020094

Pucéat, E., Joachimski, M. M., Bouilloux, A., Monna, F., Bonin, A., Motreuil, S., et al. (2010). Revised phosphate-water fractionation equation reassessing paleotemperatures derived from biogenic apatite. *Earth and Planetary Science Letters*, *298*(1–2), 135–142. https://doi.org/10.1016/j.epsl.2010.07.034

Roelofs, B., Barham, M., Cliff, J., Joachimski, M., Martin, L., & Trinajstic, K. (2017). Assessing the fidelity of marine vertebrate microfossil δ18O signatures and their potential for palaeo-ecological and -climatic reconstructions. *Palaeogeography, Palaeoclimatology, Palaeoecology*, *465*, 79–92. https://doi.org/10.1016/j.palaeo.2016.10.018

Scher, H. D., & Martin, E. E. (2006). Timing and climatic consequences of the opening of drake passage. *Science*, *312*(5772), 428–430. https://doi.org/10.1126/science.1120044

Schmidt, G. A., Bigg, G. R., & Rohling, E. J. (1999). Global Seawater Oxygen-18 Database - v1.22. Retrieved from https://data.giss.nasa.gov/o18data/

Shipley, O. N., Henkes, G. A., Gelsleichter, J., Morgan, C. R., Schneider, E. V., Talwar, B. S., & Frisk, M. G. (2021). Shark tooth collagen stable isotopes (δ15N and δ13C) as ecological proxies. *Journal of Animal Ecology*, *90*(9), 2188–2201. https://doi.org/10.1111/1365-2656.13518

Sisma-Ventura, G., Tütken, T., Peters, S. T. M., Bialik, O. M., Zohar, I., & Pack, A. (2019). Past aquatic environments in the Levant inferred from stable isotope compositions of carbonate and phosphate in fish teeth. *PLoS ONE*, *14*(7), 1–18. https://doi.org/10.1371/journal.pone.0220390

Skomal, G. B., Braun, C. D., Chisholm, J. H., & Thorrold, S. R. (2017). Movements of the white shark Carcharodon carcharias in the North Atlantic Ocean. *Marine Ecology Progress Series*, *580*, 1–16. https://doi.org/10.3354/meps12306

Spero, H. J., Bijma, J., Lea, D. W., & Bemis, B. E. (1997). Effect of seawatercarbonate concentrationon foraminiferal carbonandoxygen isotopes. *Nature*, *390*, 497–500.

Steinthorsdottir, M., Coxall, H. K., de Boer, A. M., Huber, M., Barbolini, N., Bradshaw, C. D., & Strömberg, C. A. E. (2021). The Miocene: The Future of the Past, *36*.

Steph, S., Tiedemann, R., Prange, M., Groeneveld, J., Nürnberg, D., Reuning, L., et al. (2006). Changes in Caribbean surface hydrography during the Pliocene shoaling of the Central American Seaway. *Paleoceanography*, *21*(4), 1–25. https://doi.org/10.1029/2004PA001092

Steph, S., Tiedemann, R., Prange, M., Groeneveld, J., Schulz, M., Timmermann, A., et al. (2010). Early Pliocene increase in thermohaline overturning: A precondition for the development of the modern equatorial Pacific cold tongue. *Paleoceanography*, *25*(2), 1–17. https://doi.org/10.1029/2008PA001645

Teo, S. L. H., Boustany, A., Blackwell, S., Walli, A., Weng, K. C., & Block, B. A. (2004). Validation of geolocation estimates based on light level and sea surface temperature from electronic tags. *Marine Ecology Progress Series*, *283*, 81–98. https://doi.org/10.3354/meps283081

Teter, S. M., Wetherbee, B. M., Fox, D. A., Lam, C. H., Kiefer, D. A., & Shivji, M. (2015).

Migratory patterns and habitat use of the sand tiger shark (Carcharias taurus) in the western North Atlantic. *Marine and Freshwater Research*, *66*(2), 158–169. https://doi.org/10.1071/MF14129

Tinari, A. M., & Hammerschlag, N. (2021). An ecological assessment of large coastal shark communities in South Florida. *Ocean and Coastal Management*, *211*(June), 105772. https://doi.org/10.1016/j.ocecoaman.2021.105772

Vennemann, T. W., & Hegner, E. (1998). Oxygen, strontium, and neodymium isotope composition of fossil shark teeth as a proxy for the palaeoceanography and palaeoclimatology of the Miocene northern Alpine Paratethys. *Palaeogeography, Palaeoclimatology, Palaeoecology*, *142*(3–4), 107–121. https://doi.org/10.1016/S0031-0182(98)00062-5

Vennemann, T. W., Hegner, E., Cliff, G., & Benz, G. W. (2001). Isotopic composition of recent shark teeth as a proxy for environmental conditions. *Geochimica et Cosmochimica Acta*, *65*(10), 1583–1599. https://doi.org/10.1016/S0016-7037(00)00629-3

Villafaña, J. A., Marramà, G., Klug, S., Pollerspöck, J., Balsberger, M., Rivadeneira, M., & Kriwet, J. (2020). Sharks, rays and skates (Chondrichthyes, Elasmobranchii) from the Upper Marine Molasse (middle Burdigalian, early Miocene) of the Simssee area (Bavaria, Germany), with comments on palaeogeographic and ecological patterns. *PalZ*, *94*(4), 725–757. https://doi.org/10.1007/s12542-020-00518-7

Weng, K. C., Boustany, A. M., Pyle, P., Anderson, S. D., Brown, A., & Block, B. A. (2007). Migration and habitat of white sharks (Carcharodon carcharias) in the eastern Pacific Ocean. *Marine Biology*, *152*(4), 877–894. https://doi.org/10.1007/s00227-007-0739-4

Westerhold, T., Marwan, N., Drury, A. J., Liebrand, D., Agnini, C., Anagnostou, E., et al. (2020). An astronomically dated record of Earth's climate and its predictability over the last 66 million years. *Science*, *369*(6509), 1383–1388. https://doi.org/10.1126/SCIENCE.ABA6853

Wierzbowski, H. (2021). Advances and Challenges in Palaeoenvironmental Studies Based on Oxygen Isotope Composition of Skeletal Carbonates and Phosphates. *Geosciences*, *11*(10), 419. https://doi.org/10.3390/geosciences11100419

Winkelstern, I., Surge, D., & Hudley, J. W. (2013). Multiproxy sclerochronological evidence for plio-pleistocene regional warmth: United States mid-atlantic coastal plain. *Palaios*, *28*(9), 649–660. https://doi.org/10.2110/palo.2013.p13-010r

Wu, Y., Hain, M. P., Humphreys, M. P., Hartman, S., & Tyrrell, T. (2019). What drives the latitudinal gradient in open-ocean surface dissolved inorganic carbon concentration? *Biogeosciences*, *16*(13), 2661–2681. https://doi.org/10.5194/bg-16-2661-2019

Zachos, J., Pagani, H., Sloan, L., Thomas, E., & Billups, K. (2001). Trends, rhythms, and aberrations in global climate 65 Ma to present. *Science*, *292*(5517), 686–693. https://doi.org/10.1126/science.1059412

Zeebe, R. E. (1999). An explanation of the effect of seawater carbonate concentration

on foraminiferal oxygen isotopes. *Geochimica et Cosmochimica Acta*, *63*(13–14), 2001–2007. https://doi.org/10.1016/S0016-7037(99)00091-5

Zeichner, S. S., Colman, A. S., Koch, P. L., Polo-Silva, C., Galván-Magaña, F., & Kim, S. L. (2017). Discrimination factors and incorporation rates for organic matrix in shark teeth based on a captive feeding study. *Physiological and Biochemical Zoology*, *90*(2), 257–272. https://doi.org/10.1086/689192